NASA
Technical
Paper
3118

June 1991

Aeroacoustic and Aerodynamic Applications of the Theory of Nonequilibrium Thermodynamics

W. Clifton Horne,
Charles A. Smith, and
Krishnamurty Karamcheti

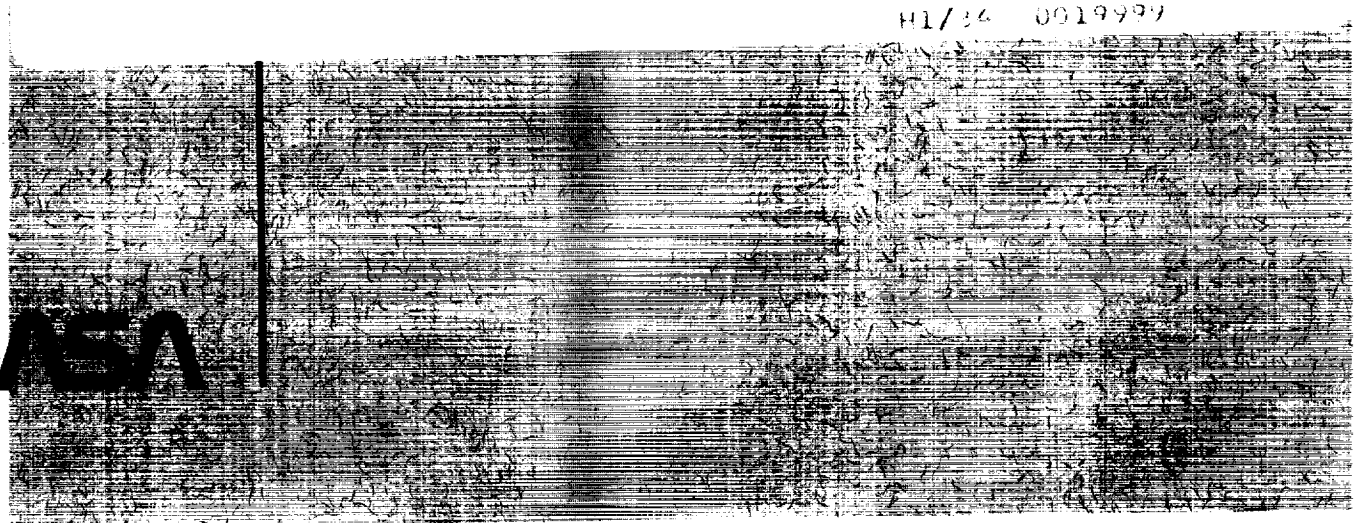

ERRATA

NASA Technical Paper 3118

AEROACOUSTIC AND AERODYNAMIC APPLICATIONS OF THE THEORY OF NONEQUILIBRIUM THERMODYNAMICS

W. Clifton Horne, Charles A. Smith, and Krishnamurty Karamcheti

June 1991

Page 5, column 1, line 32: Insert the following after equation (19): This expression is similar to Serrin's form of the Bobyleff-Forsythe equation (Serrin, J.: Mathematical Principles of Classical Fluid Mechanics. Encyclopedia of Physics, Vol. VIII/1, Fluid Dynamics I, S. Flugge and C. Truesdell, eds., Springer-Verlag, 1959, p. 251):

$$D:D = \frac{1}{2}\omega^2 + \operatorname{div}\vec{a}$$

where

$$D = \frac{1}{2}\left(\frac{\partial u_j}{\partial x_k} + \frac{\partial u_k}{\partial x_j}\right) \quad \text{and} \quad \vec{a} = \frac{D\vec{u}}{Dt}$$

For incompressible, viscous flow:

$$\vec{a} = -\nabla\left(\frac{p}{\rho}\right)$$

Page 7, column 1, line 16: Insert the following after equation (34): Equation 34 is a special case of a more general result obtained by Rayleigh, who extended Helmholz's work (Lamb, H.: Hydrodynamics. Sixth ed. Dover, 1945, p. 617). From a perturbation analysis, Rayleigh obtained the minimum dissipation condition:

$$\nabla^2\vec{V} = \nabla H, \quad H \text{ is any scalar}$$

Rayleigh stated that this condition was exclusive; flows that did not satisfy the condition were not characterized by minimum dissipation. Onsager later extended the minimum condition to all steady, linear processes that satisfied the second law of thermodynamics. Rayleigh used examples of parallel channel flow (parabolic profile) and rotational flow, as discussed by Lamb, to illustrate his minimum condition.

Page 8, column 2, line 39: The phrase "the x-derivatives" should be "the ξ-derivatives".

Page 9, column 1, line 4: The denominator of the second term in the second line of equation (48) should be squared, not cubed; the calculation used the correct expression. (See also other corrections to equation (48) below.)

Pages 9–10: The symbols x and y should be replaced with the symbols ξ and η in several equations (note that u and v are velocity components in the airfoil coordinate frame). Correct as follows:

$$\begin{aligned}\frac{\partial(u+iv)}{\partial\xi} &= \left(\frac{d(u+iv)}{dz}\right)\left(\frac{dz}{d\varsigma}\right)\left(\frac{\partial\varsigma}{\partial\xi}\right) \\ &= U\left[\frac{2a^2e^{i\alpha}}{(z+\delta)^3} - \frac{2ik_S a\sin(\alpha)}{(z+\delta)^2}\right]\left(\frac{z^2}{\left(z^2-1\right)}\right)^2 \\ &\quad + U\left[e^{-i\alpha} - \frac{a^2e^{i\alpha}}{(z+\delta)^2} + \frac{2ik_S a\sin(\alpha)}{(z+\delta)}\right] \\ &\quad \times\left(\frac{2z^3}{\left(z^2-1\right)^2} - \frac{2z^5}{\left(z^2-1\right)^3}\right)\end{aligned} \tag{48}$$

$$\Phi = \mu\left[2\left(\frac{\partial u}{\partial\xi}\right)^2 + 2\left(\frac{\partial v}{\partial\eta}\right)^2 + \left(\frac{\partial v}{\partial\xi} + \frac{\partial u}{\partial\eta}\right)^2\right] \tag{49}$$

$$\frac{\partial u}{\partial\eta} = \frac{\partial v}{\partial\xi}, \quad \frac{\partial v}{\partial\eta} = -\frac{\partial u}{\partial\xi} \tag{50}$$

$$\Phi(\xi,\eta) = 4\mu\left[\left(\frac{\partial u}{\partial \xi}\right)^2 + \left(\frac{\partial v}{\partial \xi}\right)^2\right] \tag{51}$$

$$\int_{A_v} \Phi dA_v = \left(DU + \dot{W}_{BLC}\right)/L = \frac{1}{2}\rho U^3 c C_{DE}$$

$$= 4\mu \iint_{A_v}\left[\left(\frac{\partial u}{\partial \xi}\right)^2 + \left(\frac{\partial v}{\partial \xi}\right)^2\right] d\xi\, d\eta \tag{55}$$

$$C_{DE} = \frac{8}{R}\iint_{A_v}\left[\left(\frac{\partial (u/U)}{\partial \xi}\right)^2 + \left(\frac{\partial (v/U)}{\partial \xi}\right)^2\right] d\xi\, d\eta \tag{56}$$

Page 9, column 2, line 9: After the word "points." insert the following: An inverse cubic approximation for dissipation was used in the leading edge (LE) and trailing edge (TE) regions, with a grid spacing of 0.02 in the LE region ($-2.19 < \xi < -1.81, -19 < \eta < 0.19$) and in the TE region ($1.81 < \xi < 2.19, -19 < \eta < 0.19$). The dissipation approximation was integrated analytically in the ξ direction and numerically in the η direction.

Page 10, column 1, lines 5–14: Insert a period after "zero" in line 5, and delete "and results in a net drag . . . which is drag times freestream velocity."

Page 10, column 2, line 26: Insert the following: For all the examples of incompressible and fully irrotational flow, the net drag is zero and the dissipation is due entirely to the work of the moving-surface boundary-layer control system ($\dot{W}_{BLC}$). This quantity represents the minimum power expended by an ideal airfoil. The drag of an actual airfoil can be related to this quantity by defining a boundary layer control efficiency:

$$\eta_{BLC} = \left[\frac{\left(\dot{W}_{BLC}\right)_{irrot.\ flow}}{\left(DU + \dot{W}_{BLC}\right)_{actual}}\right]_{equal\ lift,\ velocity}$$

Page 10, column 2, line 32: Insert the following: The effective drag coefficient C_{DE} as presented in the text represents a power loss coefficient, indicating boundary later control power only for the airfoil in fully irrotational flow and drag plus boundary layer control power for airfoils in rotational flow.

Issued 5-5-92

NASA Technical Paper 3118

1991

Aeroacoustic and Aerodynamic Applications of the Theory of Nonequilibrium Thermodynamics

W. Clifton Horne
and Charles A. Smith
Ames Research Center
Moffett Field, California

Krishnamurty Karamcheti
FAMU-FSU College of Engineering
Tallahassee, Florida

National Aeronautics and Space Administration
Office of Management
Scientific and Technical Information Program

NOMENCLATURE

A_B	surface of body subjected to drag force
A_V	surface bounding control volume
a	circle radius for streamlined-airfoil flow
a_0	speed of sound in undisturbed fluid
B	constant of integration
C	constant of integration
C_{DE}	effective-drag coefficient
c	airfoil chord
c	wave speed
D	airfoil drag
d_{jk}	deformation-rate tensor
$\hat{e}_\theta$	unit vector in the θ direction, cylindrical coordinates
$\vec{F}$	sum of terms in momentum equation
f, f', f"	similarity function and its derivatives
g, g', g"	auxiliary similarity function and its derivatives
h	jet nozzle height
I_{div}	cross-stream integral of velocity divergence
I_T	cross-stream integral of total dissipation
I_1	cross-stream integral of mean pressure
I_2	cross-stream integral of squared mean vorticity
I_3	cross-stream integral of the mean square of fluctuating vorticity
K	bulk viscosity coefficient
k_S	vortex strength factor
k_T	coefficient of thermal conductivity
L	torque on a cylinder
L	airfoil length
L	wall length
l	channel-wall running length
M	sum of terms in mass equation
M_j, M_k	Mach numbers in j and k directions
$\hat{n}$	unit vector normal to surface
P_T	torque power absorbed by rotating cylinder
p	pressure
$\bar{p}$	time average (mean) of pressure
p'	fluctuation in time of pressure
$\vec{q}$	heat-flow vector
R	airfoil Reynolds number
R_c	critical Reynolds number
R_δ	jet Reynolds number based on jet half-width
r	radial coordinate, cylindrical coordinate system
r_{LE}	airfoil leading-edge radius
r_{TE}	airfoil trailing-edge radius
r_0	cylinder radius (vortex-core radius)
S	system entropy
s	specific entropy (entropy per unit mass)
T	temperature
t	time
t/c	airfoil thickness-to-chord ratio
$\vec{U}$	freestream velocity vector
U_m	maximum jet velocity

u,v,w	velocity components, Cartesian coordinate system
u_i,u_j,u_k	tensor velocity components
u_θ	tangentail velocity component
$\bar{u}$	velocity vector
V	control volume
$\dot{V}_c$	channel flow rate
W	complex potential
$\dot{W}_{BLC}$	boundary-layer-control system power
w	channel width
x,y,z	position components, Cartesian coordinate system
x_i,x_j,x_k	tensor position components
z	complex position, not transformed
α	Lagrange multiplier, channel flow
α	angle of attack
α	wave number
Γ	circulation, cylindrical vortex
$\dot{\Delta}S$	rate of change in the system entropy
$\dot{\Delta}_eS$	contributions to $\dot{\Delta}S$ from external sources
$\dot{\Delta}_iS$	contributions to $\dot{\Delta}S$ from internal sources
δ	circle offset distance
δ_{jk}	Kronecker delta
$\delta_{1/2}$	jet half-width
ε	disturbance amplitude
ζ	complex position, transformed
η	similarity parameter
θ	angular coordinate, cylindrical coordinate system
λ	second coefficient of viscosity
μ	first coefficient of viscosity
ρ	density
σ	fluid stress
$\sigma_{r\theta}$	shear stress, cylindrical vortex
τ'_{jk}	viscous stress tensor
Φ	viscous dissipation function
Φ^*	dimensionless dissipation function
$\tilde{\Phi}$	modified dissipation function
$\tilde{\Phi}_I$	modified dissipation function for incompressible flow
$\tilde{\Phi}_R$	radiative component of modified dissipation function
ϕ	unsteady, complex disturbance stream function
φ	complex amplitude of the disturbance stream function
φ_i	imaginary component of the amplitude of the disturbance stream function
φ_r	real component of the amplitude of the disturbance stream function
Ω	cylinder rotation rate
ω	complex frequency
ω	vorticity
$\bar{\omega}$	time average (mean) of vorticity
ω'	fluctuation in time of vorticity
ω_i	imaginary component of complex frequency
ω_{jk}	rate-of-rotation tensor

SUMMARY

The objective of this report is to examine recent developments in the field of nonequilibrium thermodynamics associated with viscous flows, and to relate these developments to the understanding of specific phenomena in aerodynamics and aeroacoustics. A key element of the nonequilibrium theory is the principle of minimum entropy production rate for steady dissipative processes near equilibrium, and variational calculus is used to apply this principle to several examples of viscous flow. The paper begins with a review of nonequilibrium thermodynamics and its role in fluid motion. Several formulations are presented of the local entropy production rate and the local energy dissipation rate, two quantities that are of central importance to the theory. These expressions and the principle of minimum entropy production rate for steady viscous flows are used to identify parallel-wall channel flow and irrotational flow as having minimally dissipative velocity distributions. Features of irrotational, steady, viscous flow near an airfoil, such as the effect of trailing-edge radius on circulation, are also found to be compatible with the minimum principle. Finally, the minimum principle is used to interpret the stability of an initially laminar, parallel shear flow with respect to infinitesimal and finite amplitude disturbances; the results are consistent with experiment and with linearized hydrodynamic stability theory. These results suggest that a thermodynamic approach may be useful in unifying the understanding of many diverse phenomena in aerodynamics and aeroacoustics.

INTRODUCTION

The crucial role thermodynamics plays in fluid mechanics and related disciplines such as aerodynamics is indicated by the importance of the perfect gas law and the energy equation, which, together with the principles of mass and momentum conservation, form the basis of the theory of fluid motion. The gas law and the energy equation can be formulated for a system of fluid particles in thermodynamic equilibrium, a system devoid of spatial or temporal variations in material properties. For compressible flows, such as flows containing shock waves, the equilibrium approximation is still accurate locally because of the large number of particles in the smallest regions of interest.

Spatial and temporal variations in the fluid properties may become significant to the thermodynamic description of the system when the variations in thermal energy are independent of the variations in fluid pressure, such as in low-speed flow, or when the variations in fluid properties with time are large. When the flow is steady, the theory of linear nonequilibrium thermodynamics leads to several useful concepts, including the principle of minimum entropy production for near-equilibrium processes and the subsequent formulation of variational methods consistent with this principle. In certain unsteady flows that are thermodynamically far from equilibrium, such as Benard convection, the heat transfer and entropy production can be maximized.

Variational principles associated with energy dissipation of a viscous fluid have been applied with varying degrees of success. In the field of hydrodynamics, Helmholz proved that flow with negligible inertia forces is characterized by a minimum of viscous dissipation (ref. 1). Tadmor defined a minimum entropy principle in the context of stable numerical solutions of the gas dynamics equations (ref. 2). For thermal convection and turbulent flow in channels, Malkus proposed a theory based on the arguments that the smallest turbulent scales are marginally stable, and the mean and turbulent characteristics of the flow are determined by the condition that the energy dissipation is maximized (refs. 3,4). Reynolds and Tiederman contended that extrema of the dissipation function are not generally compatible with the conservation laws, and they found poor agreement between an eddy viscosity simulation of turbulent channel flow and Malkus' prediction of the association of maximum dissipation rate with neutral stability of the mean flow (ref. 5). Gage et al. argued against the existence of a general thermokinetic variational principle (ref. 6).

These efforts raise questions about (1) whether a general variational principle is applicable to problems in fluid mechanics, (2) which fluid property is to be extremized, and (3) whether a maximum or minimum of the property should be expected. These issues can be clarified by the review that follows of the results of studies of nonequilibrium thermodynamics. For a full discussion of nonequilibrium thermodynamics, the reader is referred to the treatises by Yourgrau et al. (ref. 7) and de Groot and Mazur (ref. 8).

Thermodynamic equilibrium, characterized by the absence of gradients of state variables or kinematic

variables, corresponds to a state of zero entropy production and maximum entropy. Linear nonequilibrium processes, studied by Onsager (ref. 9), are associated with nonzero gradients of system properties and are characterized by minimum entropy production or energy dissipation. This characterization specifies that the entropy production can be evaluated at every point in the fluid, and that the spatial distribution of this quantity is such that the volume integral of the entropy production is smaller for the observed spatial distribution than for any other possible distribution. The volume integral of the entropy production is also described as stationary since a small deviation from the observed distribution results in a variation of the volume integral that is on the order of the square of the deviation. The linear description applies if the generalized thermodynamic fluxes (such as heat flow or fluid deformation) are linearly related to the generalized thermodynamic forces (such as temperature gradient or viscous stress). Many near-equilibrium processes are accurately characterized as linear. Minimum entropy production for these processes can be associated with the stability of stationary or time-invariant states in the presence of fluctuations in one or more of the thermodynamic forces or fluxes.

Prigogine noted that the entropy production characteristics for nonequilibrium processes that are nonlinear or far from equilibrium can be quite different than those observed for processes close to equilibrium (ref. 10). Nonlinearity is generally associated with the generation of chaotic states from initially determinate conditions, such as the transition from laminar flow to turbulence. Prigogine (ref. 11) and Prigogine and Stengers (ref. 12) also demonstrated that nonlinearity and processes that are far from equilibrium may give rise to global organization from an initially random field, and they characterized such processes as the evolution of dissipative structures. For example, the problem of convective heat transfer can be characterized by the maximum heat transfer and entropy production that is associated, in some circumstances, with the appearance of orderly Benard convection cells (refs. 13–15). Lugt commented on the evolution of discrete vortices in shear flows as another example of these dissipative structures (ref. 16). Ziegler proposed that rates of entropy production and energy dissipation are maximized for processes far from equilibrium (ref. 17). These results suggest that maximum energy dissipation may be associated with some processes far from equilibrium, or with the transition of a system between equilibrium states.

The dissipation function in its conventional form consists of terms formed from velocity-field gradients. Vortices were cited by Lugt in reference 16 as examples of dissipative structures in fluid flow, and pressure-wave source regions may be examples as well. The first goal of this study is to formulate the dissipation function in terms directly related to these phenomena. In this context, we will derive in the next section an alternative expression of the dissipation function; its terms are associated with the processes of irreversible compression, vorticity, and convected wave propagation of density disturbances.

Many references cited in this discussion refer to the steady motion of a viscous fluid as an example of a linear, nonequilibrium process for which entropy production should be minimized. The second goal of this study is to present some specific examples of this concept. Finally, we will compare the hydrodynamic and thermodynamic stability characteristics of a viscous, parallel shear flow.

DISSIPATION FUNCTIONS FOR A NEWTONIAN FLUID

Entropy Change in a Fluid Particle System

Yourgrau et al. studied the rate of change of entropy in an open system that allows the transfer of mass and energy across system boundaries (ref. 7). For such systems, the rate of change of the system entropy, $\dot{\Delta}S$, is composed of contributions from external and internal sources:

$$\dot{\Delta}S = \dot{\Delta}_e S + \dot{\Delta}_i S \tag{1}$$

The first term, $\dot{\Delta}_e S$, represents the entropy exchange across the system boundaries by mass or heat transfer. It may be positive or negative depending on whether entropy is transferred in or out of the system. The second term, $\dot{\Delta}_i S$, represents the entropy production within the system boundaries caused by irreversible processes, such as heat conduction and viscous dissipation of energy. According to the second law of thermodynamics, it is always positive.

If we consider only viscous and thermal conduction effects, we can express equation (1) in terms of integrals over the system volume, V, bounded by the system surface, A:

$$\underbrace{\frac{\partial}{\partial t}\iiint_V \rho s\, dv}_{\dot{\Delta} S} = \underbrace{-\iint_A \frac{\vec{q}}{T}\cdot\hat{n}\, da - \iint_A \rho s\vec{u}\cdot\hat{n}\, da}_{\dot{\Delta}_e S} + \underbrace{\iiint_V \left(\frac{\Phi}{T} - \frac{\vec{q}\cdot\nabla T}{T^2}\right) dv}_{\dot{\Delta}_i S} \qquad (2)$$

The viscous dissipation function, Φ, is the inner product of the viscous stress tensor, τ'_{jk}, and the deformation-rate tensor, d_{jk}.

The surface integrals may be changed to volume integrals by using the divergence theorem. Since the equality must hold for arbitrary volumes of integration, the integrand of the volume integral satisfies the equality

$$\frac{\partial \rho s}{\partial t} = -\nabla\cdot\rho s\vec{u} - \nabla\cdot\frac{\vec{q}}{T} + \frac{\Phi}{T} - \frac{\vec{q}\cdot\nabla T}{T^2} \qquad (3a)$$

Applying the equation of mass conservation gives

$$\rho\frac{Ds}{Dt} = -\nabla\cdot\frac{\vec{q}}{T} + \frac{\Phi}{T} - \frac{\vec{q}\cdot\nabla T}{T^2} \qquad (3b)$$

We now restrict our attention to a Newtonian fluid, in which the viscous stress is linearly related to the deformation, or strain, rate,

$$\tau'_{jk} = 2\mu d_{jk} + \lambda\frac{\partial u_i}{\partial x_i}\delta_{jk} = 2\mu\tilde{d}_{jk} + K\frac{\partial u_i}{\partial x_i}\delta_{jk} \qquad (4)$$

where

$$K = \lambda + \frac{2}{3}\mu \qquad (5a)$$

$$d_{jk} = \frac{1}{2}\left(\frac{\partial u_j}{\partial x_k} + \frac{\partial u_k}{\partial x_j}\right) \qquad (5b)$$

$$\tilde{d}_{jk} = \frac{1}{2}\left(\frac{\partial u_j}{\partial x_k} + \frac{\partial u_k}{\partial x_j}\right) - \frac{1}{3}\frac{\partial u_i}{\partial x_i}\delta_{jk} \qquad (5c)$$

and the heat flow is linearly related to the temperature gradient,

$$\vec{q} = -k_T\nabla T \qquad (6)$$

The dissipation function can be written in Cartesian coordinates as

$$\Phi = \mu\left[2\left(\frac{\partial u}{\partial x}\right)^2 + 2\left(\frac{\partial v}{\partial y}\right)^2 + 2\left(\frac{\partial w}{\partial z}\right)^2 + \left(\frac{\partial v}{\partial x} + \frac{\partial u}{\partial y}\right)^2 + \left(\frac{\partial w}{\partial y} + \frac{\partial v}{\partial z}\right)^2 + \left(\frac{\partial u}{\partial z} + \frac{\partial w}{\partial x}\right)^2\right] + \lambda\left(\frac{\partial u}{\partial x} + \frac{\partial v}{\partial y} + \frac{\partial w}{\partial z}\right)^2 \qquad (7a)$$

or

$$\Phi = \mu\left[2\left(\frac{\partial u}{\partial x}\right)^2 + 2\left(\frac{\partial v}{\partial y}\right)^2 + 2\left(\frac{\partial w}{\partial z}\right)^2 + \left(\frac{\partial v}{\partial x} + \frac{\partial u}{\partial y}\right)^2 + \left(\frac{\partial w}{\partial y} + \frac{\partial v}{\partial z}\right)^2 + \left(\frac{\partial u}{\partial z} + \frac{\partial w}{\partial x}\right)^2 - \frac{2}{3}\left(\frac{\partial u}{\partial x} + \frac{\partial v}{\partial y} + \frac{\partial w}{\partial z}\right)^2\right] + K\left(\frac{\partial u}{\partial x} + \frac{\partial v}{\partial y} + \frac{\partial w}{\partial z}\right)^2 \qquad (7b)$$

Equation (3b) for a Newtonian fluid can be written as

$$\rho\frac{Ds}{Dt} = \frac{\Phi}{T} + \frac{k_T\nabla^2 T}{T^2} \qquad (8)$$

Since shear, dilatation, and heat transfer can occur independently, the second law of thermodynamics requires that the coefficients μ, K, and k_T each be positive. The second law of thermodynamics can be expressed either globally (an isolated system must exhibit zero or positive change in entropy) or locally (the viscous dissipation function must be positive everywhere and heat flows only from hot to cold regions). In the remaining discussion, entropy changes caused by heat conduction will be neglected, so the entropy production will be considered to be related only to the energy dissipation caused by viscous effects.

Alternative Forms of the Dissipation Function

The dissipation function can also be expressed in terms of physical mechanisms that dissipate energy. Using Cartesian tensor notation with the summation convention on repeated indices, Ziegler (ref. 17) wrote the dissipation function of equation (7a) in the form

$$\Phi = \lambda d_{jj}d_{kk} + 2\mu d_{jk}d_{jk} \qquad (9)$$

where d_{jk} is the fluid-deformation-rate, or strain-rate, tensor, defined by equation (5b). Jeffreys (ref. 18) rewrote equation (9) as

$$\Phi = \lambda \frac{\partial u_j}{\partial x_j} \frac{\partial u_k}{\partial x_k} + \mu \left[\frac{1}{2} \omega_{jk} \omega_{jk} + 2 \frac{\partial u_j}{\partial x_k} \frac{\partial u_k}{\partial x_j} \right] \quad (10)$$

where ω_{jk} is the rate-of-rotation tensor, defined by

$$\omega_{jk} = \left(\frac{\partial u_k}{\partial x_j} - \frac{\partial u_j}{\partial x_k} \right) \quad (11)$$

The last term in equation (10) appears in several aeroacoustic wave equations, such as that derived by Phillips (ref. 19). Horne and Karamcheti (ref. 20) have derived a different formulation of the dissipation function by adjoining functions of the conservation equations to the dissipation function of equation (10):

$$\tilde{\Phi} = \Phi - 2\mu \left\{ \nabla \cdot \vec{F} - \frac{DM}{Dt} + M \nabla \cdot \vec{u} \right\} \quad (12)$$

The symbols M and $\vec{F}$ refer to the sums of terms in the conservation equations of mass and momentum, respectively. They are defined by

$$M = \frac{\partial \rho}{\partial t} + u_j \frac{\partial \rho}{\partial x_j} + \rho \frac{\partial u_j}{\partial x_j} \quad (13)$$

and

$$\vec{F} = \rho \frac{\partial u_k}{\partial t} + \rho u_j \frac{\partial u_k}{\partial x_j} + \frac{\partial p}{\partial x_k} - \frac{\partial \tau'_{jk}}{\partial x_j} \quad (14)$$

where

$$\tau'_{jk} = \mu \left(\frac{\partial u_j}{\partial x_k} + \frac{\partial u_k}{\partial x_j} \right) + \delta_{jk} \lambda \frac{\partial u_j}{\partial x_j} \quad (15)$$

For a fluid free of sources of mass or momentum, $M = 0$ and $\vec{F} = 0$.

Expanding the terms of equation (12) individually, we obtain

$$\nabla \cdot \vec{F} = \overbrace{\frac{\partial \rho}{\partial x_k} \frac{\partial u_k}{\partial t}}^{A} + \overbrace{\rho \frac{\partial}{\partial t} \left(\frac{\partial u_k}{\partial x_k} \right)}^{B} + \overbrace{\frac{\partial \rho}{\partial x_k} u_j \frac{\partial u_k}{\partial x_j}}^{C}$$

$$+ \rho \frac{\partial u_j}{\partial x_k} \frac{\partial u_k}{\partial x_j} + \overbrace{\rho u_j \frac{\partial}{\partial x_j} \left(\frac{\partial u_k}{\partial x_k} \right)}^{D} + \frac{\partial^2 p}{\partial x_k \partial x_k}$$

$$- \frac{\partial^2 \tau'_{jk}}{\partial x_j \partial x_k} \quad (16a)$$

$$- \frac{\partial M}{\partial t} = - \overbrace{\frac{\partial^2 \rho}{\partial t^2} - \frac{\partial u_j}{\partial t} \frac{\partial \rho}{\partial x_j}}^{-A} - u_j \frac{\partial}{\partial t} \left(\frac{\partial \rho}{\partial x_j} \right) - \overbrace{\frac{\partial \rho}{\partial t} \frac{\partial u_j}{\partial x_j}}^{-E}$$

$$- \overbrace{\rho \frac{\partial}{\partial t} \left(\frac{\partial u_j}{\partial x_j} \right)}^{-B} \quad (16b)$$

$$- u_k \frac{\partial M}{\partial x_k} = - u_k \frac{\partial}{\partial x_k} \left(\frac{\partial \rho}{\partial t} \right) - \overbrace{u_k \frac{\partial u_j}{\partial x_k} \frac{\partial \rho}{\partial x_j}}^{-C} - u_j u_k \frac{\partial^2 \rho}{\partial x_j \partial x_k}$$

$$- \overbrace{u_k \frac{\partial \rho}{\partial x_k} \frac{\partial u_j}{\partial x_j}}^{-F} - \overbrace{\rho u_k \frac{\partial}{\partial x_k} \left(\frac{\partial u_j}{\partial x_j} \right)}^{-D} \quad (16c)$$

$$M \nabla \cdot \vec{u} = \overbrace{\frac{\partial \rho}{\partial t} \frac{\partial u_k}{\partial x_k}}^{E} + \overbrace{u_j \frac{\partial \rho}{\partial x_j} \frac{\partial u_k}{\partial x_k}}^{F} + \rho \frac{\partial u_j}{\partial x_j} \frac{\partial u_k}{\partial x_k} \quad (16d)$$

When terms are canceled as indicated, equation (12) becomes

$$\tilde{\Phi} = \frac{2\mu}{\rho} (2\mu + \lambda) \frac{\partial^2}{\partial x_k \partial x_k} \left(\frac{\partial u_j}{\partial x_j} \right) + (\lambda - 2\mu) \frac{\partial u_j}{\partial x_j} \frac{\partial u_k}{\partial x_k}$$

$$- \frac{2\mu}{\rho} \left(\frac{\partial^2 p}{\partial x_k \partial x_k} - u_j u_k \frac{\partial^2 \rho}{\partial x_j \partial x_k} - 2 u_k \frac{\partial^2 \rho}{\partial x_k \partial t} \right.$$

$$\left. - \frac{\partial^2 \rho}{\partial t^2} \right) + \frac{\mu}{2} \omega_{jk} \omega_{jk} \quad (17)$$

This expression, which is exact for a Newtonian fluid, accounts for three important mechanisms of energy dissipation in real flows: (1) irreversible expansion or compression of the fluid, (2) the generation and radiation of sound or shock waves, and (3) the generation of vorticity. The modified dissipation function of equation (17) is equal to the original dissipation function if the

conservation equations of mass and momentum are each satisfied, so extrema of the volume integral of equation (17) should also be compatible with the conservation equations. Although equation (17) was derived in a manner similar to the method of imposing equality constraints on variational problems, the conservation equations were not adjoined independently, so further consideration of this issue is necessary.

The radiative terms in equation (17) can be further manipulated to yield a convective wave operator acting on the density field:

$$\tilde{\Phi}_R = \frac{2\mu a_0^2}{\rho}\left\{\frac{\partial^2}{\partial x_k \partial x_k}\left(\rho - \frac{p}{a_0^2}\right) - \left(\frac{\partial^2 \rho}{\partial x_k \partial x_k} - M_j M_k \frac{\partial^2 \rho}{\partial x_j \partial x_k} - 2\frac{M_k}{a_0}\frac{\partial^2 \rho}{\partial x_k \partial t} - \frac{1}{a_0^2}\frac{\partial^2 \rho}{\partial t^2}\right)\right\} \quad (18)$$

where a_0 is the speed of sound in an undisturbed fluid, and M_j and M_k are the Mach numbers in the j and k directions. The first term occurs in Lighthill's acoustic stress tensor (ref. 21), and the second term, a convective wave operator for the density, is identical to the convective wave operator for acoustical disturbances in shear flow (ref. 22). Flows that generate and radiate acoustic energy have nonvanishing levels of viscous dissipation in the aeroacoustic source region of the flow. (Dissipation in the propagation region caused by viscosity and relaxation was studied by Meixner, as discussed by de Groot and Mazur (ref. 8).) The dissipation function should be positive everywhere, although the terms associated with outward acoustic radiation are negative, since energy is radiated away from, rather than deposited within, the aeroacoustic source region.

For incompressible flow, the dissipation function of equation (17) reduces to

$$\tilde{\Phi}_I = -\frac{2\mu}{\rho}\nabla^2 p + \mu\omega^2 \quad (19)$$

The squared-vorticity term, $\mu\omega^2$, which also appears in equation (10), is similar to the quantity enstrophy, which is one half of the vorticity squared and is of significance in atmospheric flows. Some studies have suggested that this quantity is minimized for certain atmospheric vortices (ref. 23). The squared-vorticity term is also similar to the energy dissipation in homogeneous turbulence, given by Hinze (ref. 24) and Tennekes and Lumley (ref. 25) as the viscosity times the mean square of the fluctuating vorticity.

These expressions for the dissipation function (eqs. (7a), (19)) will be used in the following sections to examine several simple flows, to determine if minimally dissipative distributions correspond to observed flows.

INCOMPRESSIBLE-FLOW DISTRIBUTIONS

The dissipation functions derived in the previous section can be used to determine whether simple, steady, viscous flows may be characterized by velocity distributions that generate stationary or minimum values of the net dissipation, as predicted by the theory of linear, nonequilibrium thermodynamics. Examples of such flows to be considered in the following sections are flow in a parallel-wall channel, unconstrained viscous flow, flow near a rotating cylinder, and flow near a streamlined airfoil.

Parallel-Wall Channel Flow

We will examine parallel channel flow, or Poiseuille flow, as a simple illustration of the method to be used throughout this discussion. For this flow, the streamwise velocity, u, is a function of the cross-stream coordinate, y, only. The viscous dissipation function given by equation (7a) reduces to

$$\Phi = \mu\left(\frac{\partial u}{\partial y}\right)^2 \quad (20)$$

The net dissipation per unit length per unit width is given by

$$\frac{1}{lw}\int_V \Phi \, dv = \mu \int_{y_1}^{y_2}\left(\frac{\partial u}{\partial y}\right)^2 dy \quad (21)$$

where l and w are the channel-wall running length and channel width, respectively. The flow rate per unit width through the channel is given by

$$\frac{1}{w}\dot{V}_c = \int_{y_1}^{y_2} u \, dy \quad (22)$$

Possible extrema of the integral in equation (21), subject to constant channel flow rate, are found as solutions of the Euler-Lagrange equation,

$$\frac{\partial f}{\partial u} - \frac{\partial}{\partial y}\left(\frac{\partial f}{\partial u'}\right) = 0 \quad (23)$$

where

$$u' = \frac{\partial u}{\partial y} \tag{24a}$$

$$f = \mu\left(\frac{\partial u}{\partial y}\right)^2 + \alpha u \tag{24b}$$

Here, α is a Lagrange multiplier adjoining the integrand of the flow-rate constraint to the extremizing function. For this example, evaluation of the Euler-Lagrange equation yields the expression

$$\alpha = 2\mu\frac{\partial^2 u}{\partial y^2} \tag{25}$$

The net dissipation is stationary for the parabolic profile

$$u(y) = \frac{\alpha}{2\mu}y^2 + By + C \tag{26}$$

where B and C are constants of integration. This profile corresponds to a minimum of the dissipation function, according to Legendre's test (ref. 26), since

$$\frac{\partial^2 f}{\partial u' \partial u'} = +2 \tag{27}$$

Unconstrained Viscous Flow

The preceding example incorporated a constraint on the net flow rate. In addition, the equation of mass was satisfied by the specified restrictions on the velocity field. We now consider general incompressible viscous flows that satisfy no constraints other than the integrability and differentiability requirements of a variational analysis.

The dissipation function of equation (7a), when simplified for incompressible flow, becomes

$$\Phi = \mu\left[2u_x^2 + 2v_y^2 + 2w_z^2 + \left(v_x + u_y\right)^2 + \left(w_y + v_z\right)^2 + \left(u_z + w_x\right)^2\right] \tag{28}$$

where the subscripts x, y, and z refer to partial differentiation. We will consider various circumstances under which the integral of the dissipation function (the net dissipation) over a flow region may be stationary.

The net dissipation may be expressed in integral form as

$$\int_V \Phi dv = \iiint_V \Phi\left(u_x, u_y, u_z, v_x, v_y, v_z, w_x, w_y, w_z\right) dx\, dy\, dz \tag{29}$$

Velocity distributions that generate a stationary or minimum value of the net dissipation must satisfy the Euler-Lagrange equations (ref. 26). For three dependent variables (u, v, w) and three independent variables (x, y, z) these equations are

$$\frac{\partial\Phi}{\partial u} - \frac{\partial}{\partial x}\left(\frac{\partial\Phi}{\partial u_x}\right) - \frac{\partial}{\partial y}\left(\frac{\partial\Phi}{\partial u_y}\right) - \frac{\partial}{\partial z}\left(\frac{\partial\Phi}{\partial u_z}\right) = 0 \tag{30a}$$

$$\frac{\partial\Phi}{\partial v} - \frac{\partial}{\partial x}\left(\frac{\partial\Phi}{\partial v_x}\right) - \frac{\partial}{\partial y}\left(\frac{\partial\Phi}{\partial v_y}\right) - \frac{\partial}{\partial z}\left(\frac{\partial\Phi}{\partial v_z}\right) = 0 \tag{30b}$$

$$\frac{\partial\Phi}{\partial w} - \frac{\partial}{\partial x}\left(\frac{\partial\Phi}{\partial w_x}\right) - \frac{\partial}{\partial y}\left(\frac{\partial\Phi}{\partial w_y}\right) - \frac{\partial}{\partial z}\left(\frac{\partial\Phi}{\partial w_z}\right) = 0 \tag{30c}$$

No boundary conditions or other constraints have been imposed, although such constraints may be adjoined with Lagrange multipliers, as in parallel channel flow. The terms in equation (30a) are evaluated as

$$\frac{\partial\Phi}{\partial u} = 0 \tag{31a}$$

$$\frac{\partial\Phi}{\partial u_x} = 4\mu\frac{\partial u}{\partial x}; \quad \frac{\partial}{\partial x}\left(\frac{\partial\Phi}{\partial u_x}\right) = 4\mu\frac{\partial^2 u}{\partial x^2} \tag{31b}$$

$$\frac{\partial\Phi}{\partial u_y} = 2\mu\left(\frac{\partial v}{\partial x} + \frac{\partial u}{\partial y}\right); \quad \frac{\partial}{\partial y}\left(\frac{\partial\Phi}{\partial u_y}\right) = 2\mu\left(\frac{\partial^2 v}{\partial x \partial y} + \frac{\partial^2 u}{\partial y^2}\right) \tag{31c}$$

$$\frac{\partial\Phi}{\partial u_z} = 2\mu\left(\frac{\partial u}{\partial z} + \frac{\partial w}{\partial x}\right); \quad \frac{\partial}{\partial z}\left(\frac{\partial\Phi}{\partial u_z}\right) = 2\mu\left(\frac{\partial^2 u}{\partial z^2} + \frac{\partial^2 w}{\partial z \partial x}\right) \tag{31d}$$

Summing these terms and rearranging give the Euler-Lagrange equation for u,

$$2\mu\nabla^2 u + 2\mu\frac{\partial}{\partial x}(\nabla\cdot\vec{u}) = 0 \qquad (32)$$

Adding the Euler-Lagrange equations for the three components gives the vector equation

$$2\mu\nabla^2\vec{u} + 2\mu\nabla(\nabla\cdot\vec{u}) = 0 \qquad (33)$$

The presence of the second term in equation (33) indicates that velocity distributions that generate stationary values of the net dissipation do not necessarily satisfy the conservation equations, a concern raised by Gage et al. (ref. 6) and Reynolds and Tiederman (ref. 5). Extrema could be constrained to satisfy the conservation equations by adjoining the equations to the dissipation function with influence functions. Instead, we impose conservation of mass by setting the second term equal to zero. The net dissipation is then stationary for velocity distributions that satisfy

$$\nabla^2\vec{u} = 0 \qquad (34)$$

This condition is equivalent to the vanishing of the viscous-force vector term in the momentum equation for incompressible flow,

$$\rho\frac{D\vec{u}}{Dt} = -\nabla p + \mu\nabla^2\vec{u} \qquad (35)$$

This condition is also equivalent to a zero value for the curl of the vorticity field throughout the flow; this can be seen with the vector identity

$$\nabla^2\vec{u} = \nabla(\nabla\cdot\vec{u}) - \nabla\times(\nabla\times\vec{u}) \qquad (36)$$

The dissipation function is zero for the case of uniform rotation, since the fluid deformation is zero. The net dissipation is also stationary for velocity distributions that are irrotational. The viscous force on a volume element of fluid is proportional to the divergence of the stress and is zero for irrotational flow. However, the viscous stress, and hence the dissipation, are not generally zero for regions in a viscous fluid where the flow is irrotational. An analogous situation is found in the dissipative process of steady heat flow within a conducting solid, where the irrotational heat flux, $\vec{q}$, is proportional to the gradient of the scalar temperature, T. In the following sections, we examine two familiar flows with regard to their descriptions as irreversible thermodynamic processes.

Flow Near a Rotating Cylinder

The incompressible flow near a hollow rotating cylinder is a special case of flow with regions of solid rotational and irrotational motion. It is described in cylindrical coordinates by

$$\vec{u} = u_\theta(r)\hat{e}_\theta \qquad (37)$$

For this axisymmetric tangential flow, the viscous dissipation function of equation (7a) reduces to

$$\Phi(r) = \mu\left(\frac{\partial u_\theta}{\partial r} - \frac{u_\theta}{r}\right)^2 \qquad (38)$$

and the Euler-Lagrange equation for the net dissipation reduces to the Euler equation,

$$r^2\frac{d^2u_\theta}{dr^2} + r\frac{du_\theta}{dr} - u_\theta = 0 \qquad (39)$$

The two solutions are

$$u_\theta \propto r, r^{-1} \qquad (40)$$

These two solutions represent respectively the rotational core inside the cylinder and the potential region of a columnar vortex outside the cylinder. Both solutions represent minimum dissipation conditions, as in the channel flow.

Integrated contributions to the overall dissipation rate in the field of a cylinder with radius r_0 and circulation Γ are given in table 1. As can be seen, the net dissipation in the rotational core is zero, while the irrotational outer flow has a net positive dissipation. The tangential acceleration

Table 1. Velocity distribution and net dissipation in a steady vortex

Region	$u_\theta(r)$	$\iint \Phi\, r\,dr\,d\theta$
$0 < r < r_0$	$+\frac{\Gamma r}{2\pi r_0^2}$	0
$r_0 < r < \infty$	$+\frac{\Gamma}{2\pi r}$	$+\frac{\mu\Gamma^2}{\pi r_0^2}$

is zero throughout the flow, except at the boundary at r_0. A steady tangential stress is required at this location (provided by a thin rotating cylinder, for example) to maintain a steady flow. The net dissipation in the outer region is identical to the torque power absorbed by the rotating cylinder, since the shear stress at the cylinder wall is given by

$$\sigma_{r\theta}(r_0) = \mu\left(\frac{\partial u_\theta}{\partial r} - \frac{u_\theta}{r}\right)\Bigg|_{r_0} = -\frac{\mu\Gamma}{\pi r_0^2} \tag{41}$$

The cylinder torque is then given by

$$L = -\int_0^{2\pi} \sigma_{r\theta}(r_0)\, r_0^2\, d\theta = 2\mu\Gamma \tag{42}$$

This, combined with the cylinder rotation rate,

$$\Omega = \frac{u_\theta(r_0)}{r_0} = \frac{\Gamma}{2\pi r_0^2} \tag{43}$$

gives the torque power absorbed by the rotating cylinder,

$$P_T = L\Omega = \frac{\mu\Gamma^2}{\pi r_0^2} \tag{44}$$

In this example, the stationary dissipation is associated with either uniform or irrotational motion, as in unconstrained viscous flow. Yates and Donaldson (ref. 27) and Greene (ref. 28) have also considered energy dissipation in vortices in their analyses of induced drag.

Flow Near a Streamlined Airfoil

Another important example of viscous irrotational flow is the low-speed flow of a real fluid over a streamlined object such as an airfoil. At a sufficiently high Reynolds number, in the absence of separation, the viscous-flow effects are confined to a thin boundary layer near the surface, a fact first utilized by Prandtl in his boundary layer theory. As von Karman noted in 1941 (ref. 29):

> One of the most surprising developments in modern fluid mechanics is the successful application of the theory of potential motion of ideal incompressible fluids to the actual flow of air around airfoils and streamlined bodies. A few decades ago the potential theory was considered a purely mathematical discipline. Later it was understood that it might be a valuable guide for understanding of the general laws which govern the lift, moment, induced drag, etc. of airfoils. However, as aerodynamical design became more refined, it was found that the quantitative predictions of the theory are of a remarkable accuracy in spite of its idealized conception.

The high degree of correspondence between associated viscous and inviscid flows implies that for many flows, viscous effects are confined to a thin layer adjacent to a moving surface, and that large regions of the real flow sufficiently far from boundary surfaces are irrotational. In this section we evaluate the distribution of the viscous dissipation function in the vicinity of a streamlined airfoil.

The airfoil flows investigated in this study were generated by mapping an offset circle in the z-plane to a streamlined airfoil shape in the ζ-plane with the conformal transformation

$$\zeta = z + \frac{1}{z} \tag{45}$$

The radius of the circle in the z-plane is a, centered at $z = -\delta$. A sharp trailing edge is generated if $a = 1 + \delta$. A round trailing edge is generated if $a > 1 + \delta$. The circle in figure 1 maps to an airfoil with a chord length of approximately 4. The complex potential, W, caused by a doublet, a variable-strength vortex, and a uniform stream of speed U inclined at angle α can be derived from the expression given by Abbot and von Doenhoff (ref. 30),

$$W = U\left\{(z+\delta)e^{-i\alpha} + \frac{a^2}{(z+\delta)}e^{i\alpha} + 2ik_S a\sin(\alpha) \times \ln\left[\frac{(z+\delta)e^{-i\alpha}}{a}\right]\right\} \tag{46}$$

The vortex strength, k_S, is equal to 1 when the separation streamline departs from the airfoil trailing edge, and $k_S = -1$ for stagnation at the airfoil leading edge. For sharp trailing-edge airfoils in an inviscid fluid, the Kutta condition requires that $k_S = 1$ to avoid infinite velocities at the trailing edge. The velocity and the x-derivatives of the velocity components are given by

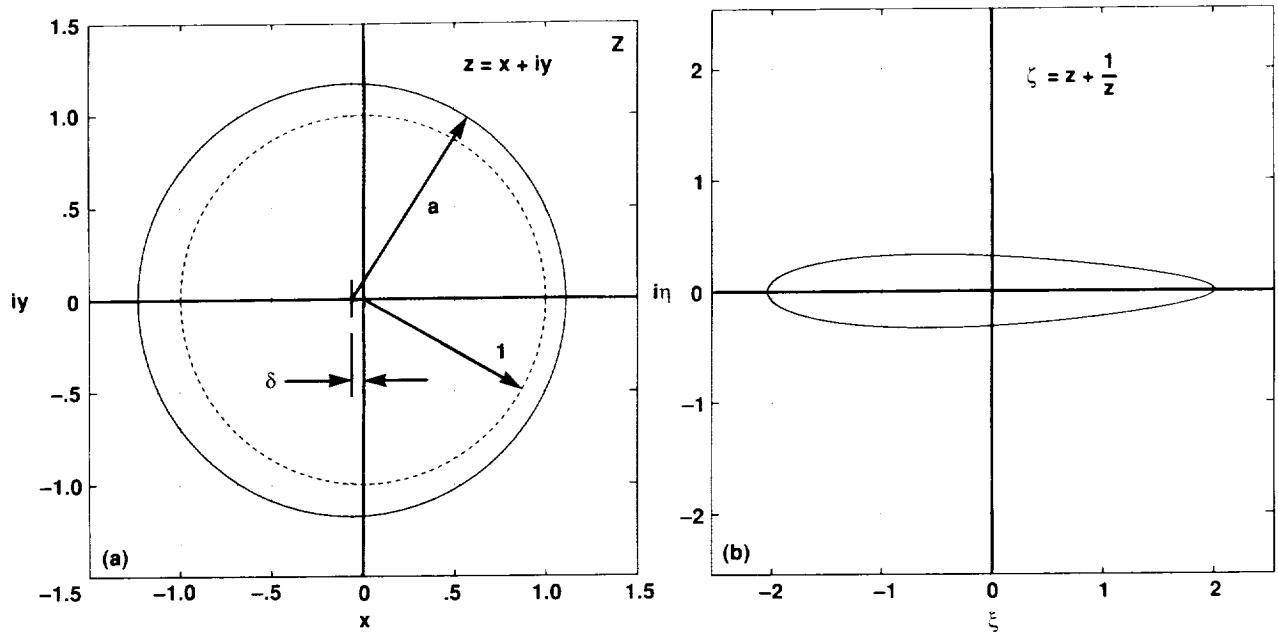

Figure 1. *(a) Cylindrical flow in z coordinate system. (b) Airfoil in transformed (ζ) coordinate system.*

$$u+iv=\frac{dW}{dz}\frac{dz}{d\varsigma}$$

$$=U\left[e^{-i\alpha}-\frac{a^2e^{i\alpha}}{(z+\delta)^2}+\frac{2ik_S a\sin(\alpha)}{(z+\delta)}\right]\left(\frac{z^2}{z^2-1}\right) \quad (47)$$

$$\frac{\partial(u+iv)}{\partial x}=\left(\frac{d(u+iv)}{dz}\right)\left(\frac{dz}{d\varsigma}\right)\left(\frac{\partial\varsigma}{\partial x}\right)$$

$$=U\left[\left(\frac{2a^2e^{i\alpha}}{(z+\delta)^3}\right)-\frac{2ik_S a\sin(\alpha)}{(z+\delta)^3}\right]\left(\frac{z^2}{\left(z^2-1\right)}\right)^2$$

$$+U\left[e^{-i\alpha}-\frac{a^2e^{i\alpha}}{(z+\delta)^2}+\frac{2ik_S a\sin(\alpha)}{(z+\delta)}\right]$$

$$\times\left(\frac{2z^3}{\left(z^2-1\right)^2}-\frac{2z^5}{\left(z^2-1\right)^3}\right) \quad (48)$$

For an incompressible, two-dimensional flow, the dissipation function reduces to

$$\Phi=\mu\left[2\left(\frac{\partial u}{\partial x}\right)^2+2\left(\frac{\partial v}{\partial y}\right)^2+\left(\frac{\partial v}{\partial x}+\frac{\partial u}{\partial y}\right)^2\right] \quad (49)$$

If the flow is irrotational as well as incompressible and two-dimensional, then

$$\frac{\partial u}{\partial y}=\frac{\partial v}{\partial x},\quad \frac{\partial v}{\partial y}=-\frac{\partial u}{\partial x} \quad (50)$$

so the dissipation function becomes

$$\Phi(x,y)=4\mu\left[\left(\frac{\partial u}{\partial x}\right)^2+\left(\frac{\partial v}{\partial x}\right)^2\right] \quad (51)$$

The dissipation can be nondimensionalized using the chord, the viscosity, and the speed:

$$\Phi^*=\frac{c^2\Phi}{\mu U^2} \quad (52)$$

The dissipation function thus obtained was evaluated on a square grid with a spacing of 0.10 between grid points. Figure 2 illustrates the streamlines and contours of constant dissipation in the vicinity of a Joukouski-type airfoil, with boundary layers excluded. The irrotational flow model corresponds to a high degree to the associated real flow, provided the Reynolds number is sufficiently large and no regions of separated flow are present. The irrotational model is even more accurate if the real airfoil is provided with a moving-surface boundary-layer-control system that can adjust the tangential velocity distribution over the airfoil surface to match the distribution predicted by the inviscid theory. This method was used by Yates to study unsteady airfoil flow (ref. 31). The thin boundary layer itself is a good approximation of such a control system.

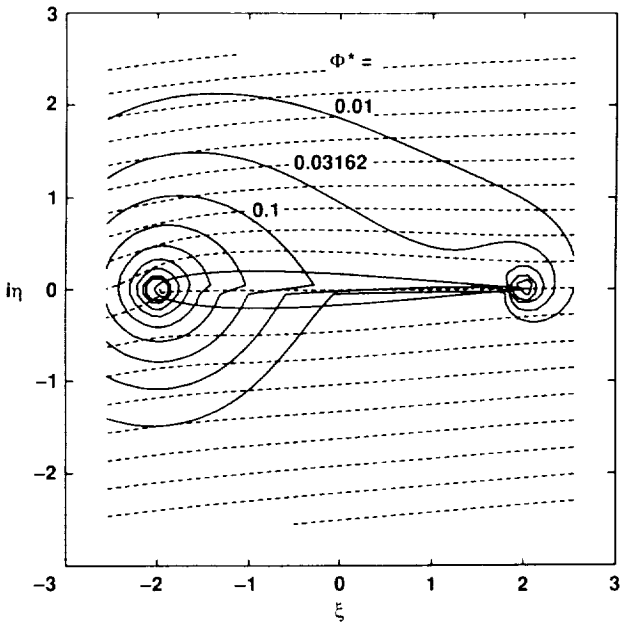

Figure 2. *Symmetrical airfoil in transformed coordinate system, t/c = 0.1, α = 0.1 rad; streamlines are dashed lines and contours of dimensionless dissipation are solid lines.*

As mentioned in the section on unconstrained viscous flow, the viscous force per unit volume in the fluid, which is proportional to the divergence of the stress, is zero throughout the irrotational region. The viscous stress, however, is not zero and results in a net drag on the airfoil even if the boundary layer is absent (assuming the no-slip condition is satisfied with a moving-surface boundary-layer control). This drag can be computed by integrating the streamwise component of the dot product of the viscous stress with the outward normal vector around a control surface such as the airfoil surface. The drag can also be found by using the energy equation; the volume integral of energy dissipation can be set equal to the drag power, which is drag times freestream velocity. Lagerstrom derived an expression for the drag power DU (ref. 32),

$$DU = \iint_{A_v} \rho \frac{\left|\vec{u}-\vec{U}\right|^2}{2} \vec{u}\cdot\hat{n}\,da - \iint_{A_v} \sigma\cdot\left(\vec{u}-\vec{U}\right)\cdot\hat{n}\,da + \iiint_{V} \sigma : \nabla\vec{u}\,dv + \iint_{A_B} \sigma\cdot\vec{u}\cdot\hat{n}\,da \qquad (53)$$

where

A_v is the surface bounding the control volume

A_B is the surface of the body subjected to drag force

$\vec{U}$ is the freestream velocity

V is the control volume

σ is the fluid stress

The terms on the right-hand side of equation (53) account for, in order, (1) net kinetic energy transfer out of the control volume, from wakes or trailing vortices, (2) stress work on the control surfaces, (3) stress work within the control volume, and (4) stress work on the surface of the body subjected to the drag force. The last term is zero if the body surface is motionless, but nonzero if the surface is moving. For the case of two-dimensional flow with negligible wakes or vortex, this expression can be simplified to

$$DU + \dot{W}_{BLC} = \iiint_{V} (p\nabla\cdot\vec{u} + \Phi)dv \qquad (54)$$

where $\dot{W}_{BLC}$ is equal to the negative of the fourth term of equation (53). The right-hand side of equation (54) is equal to the third term of equation (53). For incompressible flow, the effective drag power per unit length, $\left(DU + \dot{W}_{BLC}\right)/L$, is the surface integral of the dissipation,

$$\int_{A_v} \Phi dA_v = \left(DU + \dot{W}_{BLC}\right)/L = \frac{1}{2}\rho U^3 c\, C_{DE} = 4\mu \iint_{A_v} \left[\left(\frac{\partial u}{\partial x}\right)^2 + \left(\frac{\partial v}{\partial x}\right)^2\right] dx\,dy \qquad (55)$$

where c is the airfoil chord and L is the airfoil length. This gives an expression for the effective drag coefficient,

$$C_{DE} = \frac{8}{R}\iint_{A_v} \left[\left(\frac{\partial(u/U)}{\partial x}\right)^2 + \left(\frac{\partial(v/U)}{\partial x}\right)^2\right] dx\,dy \qquad (56)$$

where the Reynolds number is $R = \rho Uc/\mu$. The variation of C_{DE} with R for two zero-incidence airfoils that have different thickness ratios is compared in figure 3 with that of a flat plate that has boundary layers on both sides.

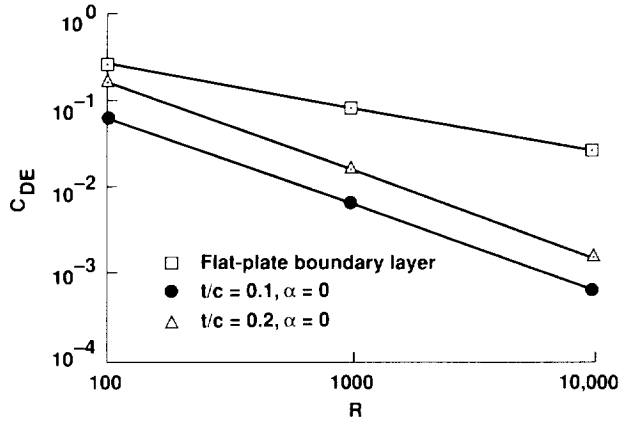

Figure 3. Zero-incidence effective-drag coefficient vs. Reynolds number for a flat-plate boundary layer (two sides) and for symmetrical airfoils (boundary-layer drag excluded on airfoils).

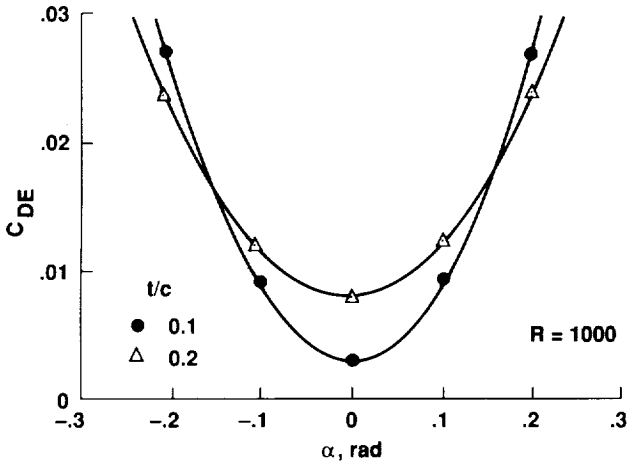

Figure 4. Variation of effective-drag coefficient with angle of attack, R = 1000.

The variation of the effective-drag coefficient with angle of attack is shown in figure 4 for airfoil thickness-to-chord ratios of 0.1 and 0.2. The effective-drag coefficient is minimized at zero incidence and increases as the square of the incidence angle, with the higher rate of increase associated with the airfoil that has the lower thickness-to-chord ratio. The region of highest flow curvature and dissipation is situated at the airfoil leading edge, as seen in figure 2.

Both the trailing-edge velocity and the net dissipation obtain infinite values if the airfoil circulation is not sufficient to maintain the separation streamline at the airfoil trailing edge. The association between net dissipation and trailing-edge streamline location can be examined further

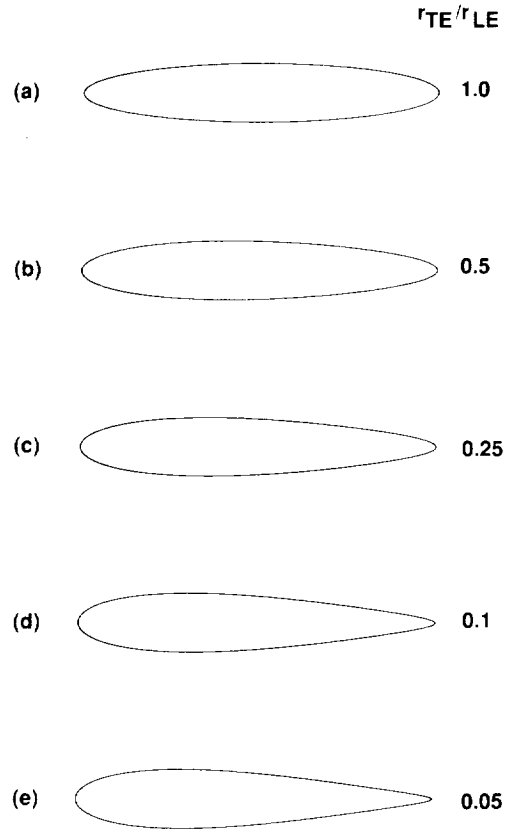

Figure 5. Airfoil section profiles with rounded trailing edges; r_{TE}/c is (a) 0.0068, (b) 0.0045, (c) 0.0027, (d) 0.0013, (e) 0.0007.

by considering the hypothetical case of continuously adjustable circulation around airfoils with rounded trailing edges (and with moving-surface boundary-layer treatment, as already discussed in this section).

Five 16.4%-thick, rounded-trailing-edge airfoil profiles were considered for this study, with trailing-edge radius-to-chord ratios of 0.0068, 0.0045, 0.0027, 0.0013, and 0.0007 (fig. 5). The geometrical parameters for these profiles are given in table 2.

The net dissipation at an incidence of 0.1 rad was found by evaluating the velocity derivatives analytically and integrating numerically, as described earlier in this section. The variation in effective drag coefficient with circulation for these airfoils at R = 1000 is shown in figure 6. For the elliptical airfoil (case 1), the net dissipation is minimized for zero circulation. The circulation corresponding to minimum net dissipation increases as the trailing-edge radius, r_{TE}, is reduced relative to the leading-edge radius, r_{LE} (fig. 6).

Table 2. Parameters for rounded-trailing-edge airfoil

Parameter	Case				
	1	2	3	4	5
radius, a	1.18	1.178	1.172	1.165	1.160
offset, δ	0.000	0.033	0.0613	0.090	0.105
LE[a] radius	0.0275	0.0368	0.0441	0.0518	0.0551
TE[b] radius	0.0275	0.0184	0.0110	0.0052	0.0029
r_{TE}/r_{LE}	1.0	0.500	0.249	0.101	0.0521
r_{TE}/c	0.0068	0.0045	0.0027	0.0013	0.0007

[a]LE = leading edge
[b]TE = trailing edge

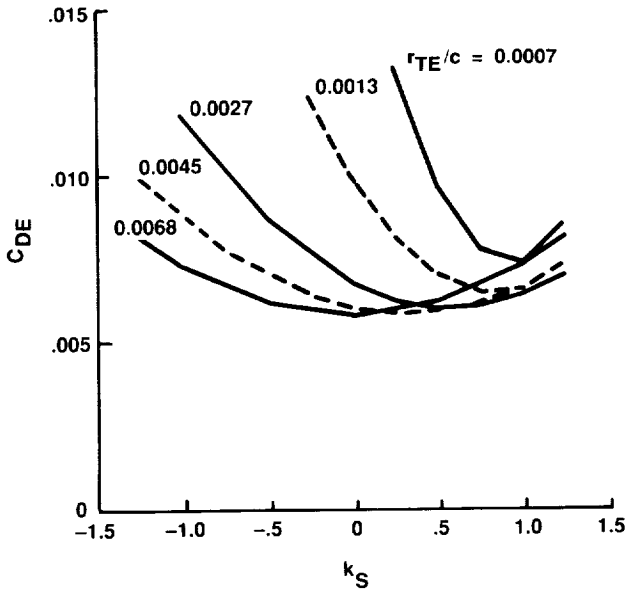

Figure 6. Drag coefficient vs. circulation coefficient; R = 1000, t/c = 0.164, α = 0.1 rad.

Streamlines and contours of constant dimensionless dissipation for full circulation (trailing-edge separation) and for circulation corresponding to minimum dissipation for the third case are shown in figure 7. For minimum dissipation conditions, the rear separation point moves rearward and the separation-stream angle decreases, as the trailing-edge radius decreases. Figure 8 illustrates how the k_S needed for minimum dissipation varies with r_{TE}/r_{LE}; this variation is nearly linear on a semilog plot. These results suggest that the familiar circulation condition for airfoils with sharp trailing edges can be approached in the limit as the trailing-edge radius vanishes. The results also suggest that the minimum dissipation condition associated with thermodynamic stability is sufficient to uniquely determine the circulation for airfoils with finite trailing-edge radii.

Attempts to compare these results with experiment must take into account the presence of the boundary layer and the zones of separation near the rounded trailing edge. For an airfoil with boundary layers, terms associated with r_{TE}/r_{LE} should have an effect of order 1/R, while terms associated with the ratio of trailing-edge radius to boundary-layer thickness will have a stronger effect, of order $1/\sqrt{R}$. Thwaites notes that the Kutta condition, which is required to avoid a singularity at the trailing edge of an airfoil in an inviscid fluid and which uniquely determines the value of circulation, has no counterpart in the case of viscous flow. Thwaites suggests a circulation condition for airfoils in viscous flow as the condition that the rear separation streamlines originate from the trailing edge at an angle that lies between the extensions of the upper and lower trailing-edge surfaces (ref. 33).

These results do not demonstrate that the entire field (irrotational regions and boundary layers) of a real viscous flow satisfies a condition of stationary dissipation; however, the value of the dissipation function for any irrotational region will be much less than the value in rotational regions. Consequently, a condition of minimum net dissipation in a real flow may correspond to the establishment of irrotational flow to the largest extent possible.

This analysis can be extended to include the effects of boundary layers, if desired. The association between thermodynamic stability and minimum net dissipation can also be extended to examine problems of hydrodynamic stability, as will be seen in the next section.

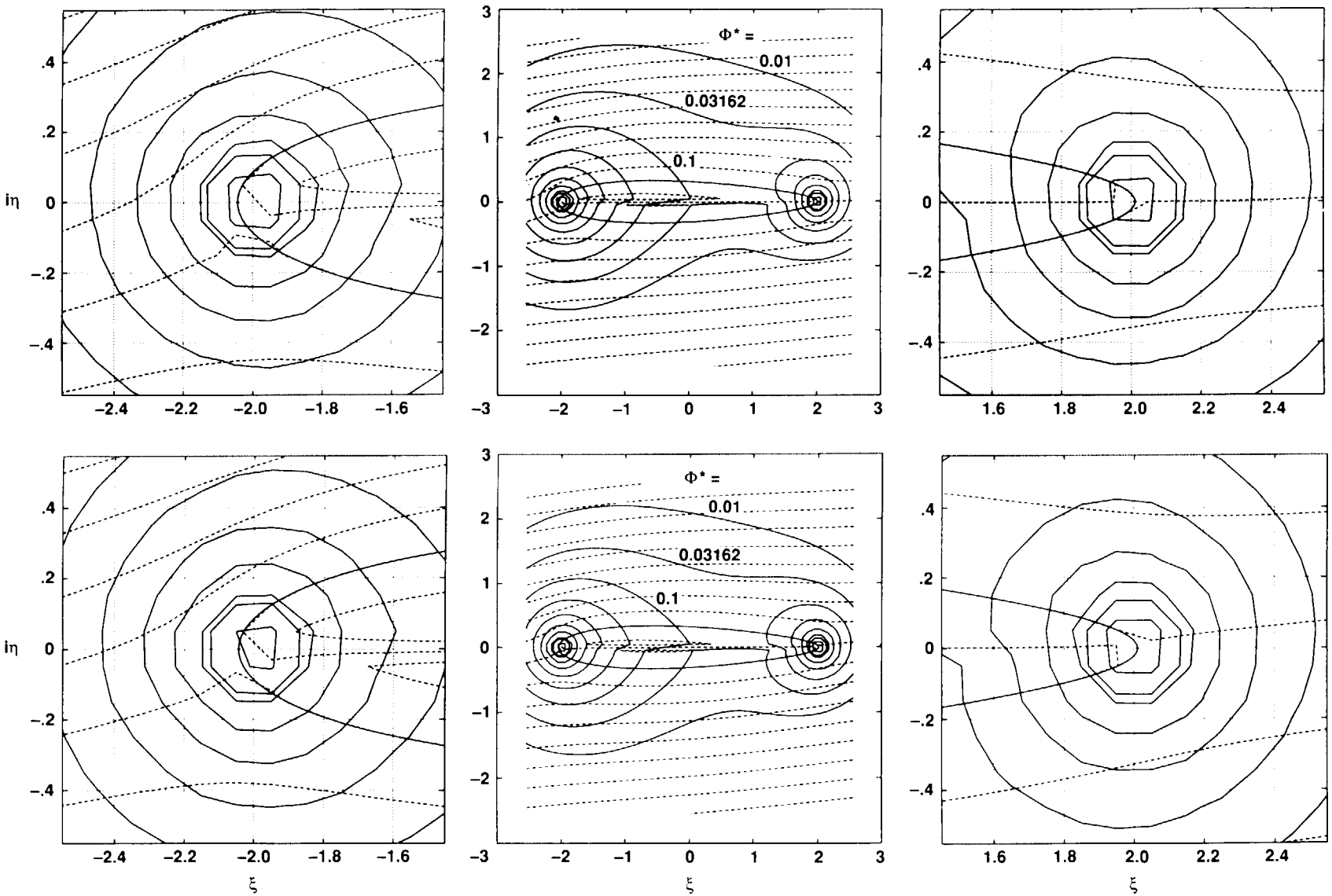

Figure 7. *Streamlines and dissipation contours in transformed coordinate system, full circulation (upper) and minimum drag circulation (lower);* $r_{TE}/c = 0.0027$, k_s *for minimum dissipation = 0.570.*

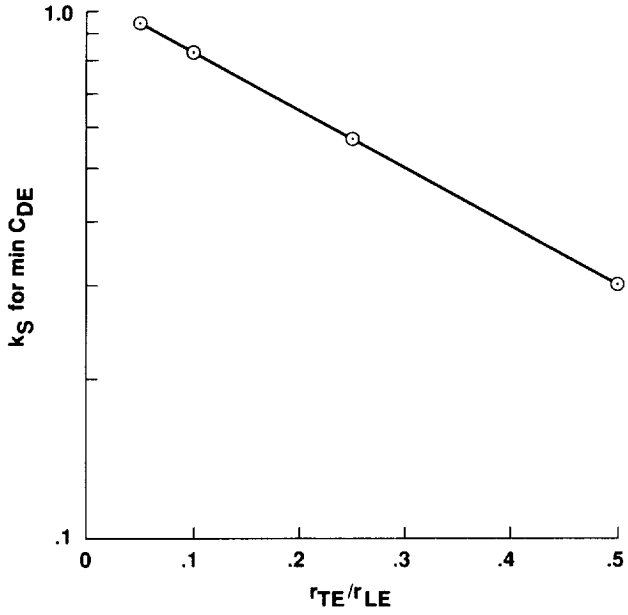

Figure 8. Circulation coefficient for minimum drag vs. r_{TE}/r_{LE}; $\alpha = 0.1$, $t/c = 0.164$.

HYDRODYNAMIC AND THERMODYNAMIC STABILITY CHARACTERISTICS OF A LAMINAR WALL JET

The initial stages of the transition of laminar flow to turbulence have been extensively studied by means of linearized hydrodynamic stability theory. This analysis has been performed for many two-dimensional, parallel shear flows, such as the boundary layer, channel flow, the free jet (ref. 34), and the wall jet (refs. 35,36). The analysis has also been extended to nonparallel flows, three-dimensional flows, and compressible flows. In general, the theory predicts that many laminar flows are stable below a critical Reynolds number, R_c, whose value depends strongly on the velocity profile. Below R_c, disturbances are damped. Above R_c, disturbances are amplified exponentially in either space or time at a rate that depends on the disturbance frequency. At any $R > R_c$, there is a frequency corresponding to the maximum amplification rate; this frequency is comparable to the experimentally observed frequency of unforced disturbances in the shear flow. Experimental disturbances in shear flows with initially low turbulence levels exhibit good agreement with linearized hydrodynamic stability theory in regions where the disturbances are amplified through several orders of magnitude. At high disturbance levels, the flow may undergo secondary instabilities and a transition to turbulence.

Viscous laminar flow may also be considered an open thermodynamic system. Energy transfers within the flow in the forms of heat conduction and energy dissipation through viscous stress are governed by the first and second laws of thermodynamics, as discussed in the introduction. If gradients in mean velocity exist within the flow, the system is not in thermodynamic equilibrium and the entropy production is nonnegligible. Under certain restrictions, the second law of thermodynamics implies that the thermodynamic state is stable when the entropy production is minimized (ref. 7). This thermodynamic stability condition has been used to examine the hydrodynamic stability of fluid motions such as pipe Poiseuille flow (ref. 37), thermal (Benard) convection (ref. 38), and transonic flow (ref. 39). However, the understanding of the extent of the correspondence between hydrodynamic and thermodynamic stability of fluid motion is not complete and would benefit from further clarification. To this end, a simple numerical illustration was generated from the results published by Chun and Schwartz of a stability analysis of a laminar wall jet (ref. 35). This exercise is described in the next section.

Wall-Jet Hydrodynamic Stability

In their stability analysis of the laminar wall jet, Chun and Schwarz predicted a critical Reynolds number of 58, with amplified disturbances in the form of a double vortex row similar to a Karman vortex street adjacent to the wall. They considered only temporally amplified disturbances, with real wave numbers and complex frequencies. Tsuji et al. confirmed the Chun and Schwartz results with a study that also examined spatially amplified disturbances (real frequencies and complex wave numbers) and verified the prediction with experiment (ref. 36).

The mean velocity field considered in these studies, as well as in the present investigation, is a parallel flow derived from the Glauert similarity solution (ref. 40):

$$u = 3.1749 U_m f' \tag{57a}$$

$$v = 0 \tag{57b}$$

$$y / \delta_{1/2} = 0.3955\eta \tag{57c}$$

where

$$\eta = \ln\left[\frac{\left(1+g+g^2\right)^{1/2}}{(1-g)}\right] + \sqrt{3}\tan^{-1}\left[\frac{\sqrt{3}g}{(2+g)}\right] \tag{58a}$$

$$f = g^2, \quad f' = 2gg', \quad g' = \frac{1}{3}\left(1 - g^3\right) \tag{58b}$$

$$f = f(\eta), \quad g = g(\eta) \tag{58c}$$

Profiles of the velocity and its first derivative are plotted in figure 9. The disturbance stream function takes the form of a convecting wave,

$$\phi(x,y,t) = \varphi(y)\exp[i\alpha(x - ct)] \tag{59}$$

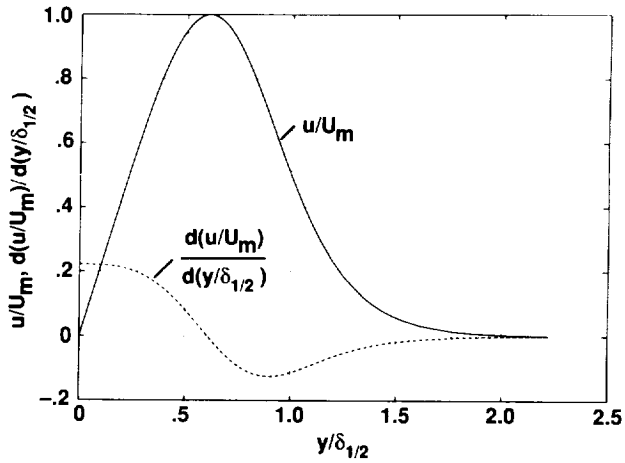

Figure 9. *Profiles of the wall-jet mean velocity and its first derivative.*

The disturbance stream function satisfies the Orr-Somerfeld equation, the boundary conditions at the wall, and the conditions far from the wall. The boundary conditions, which define an eigenvalue problem, allow the complex frequency, $\omega = \alpha c$, to be determined as a function of the Reynolds number, R_δ, and the real wave number, α. The plot by Tsuji and Morikawa (ref. 36) of the imaginary component ω_i of the complex frequency is reproduced in figure 10. Chun and Schwarz presented the real and imaginary components of the disturbance stream function for three conditions,

1. $\alpha = 1$, $R_\delta = 30$ (stable)

2. $\alpha = 1$, $R_\delta = 58.2$ (neutral)

3. $\alpha = 1$, $R_\delta = 150$ (unstable)

These conditions are indicated in figure 10 and the stream function components are presented in figure 11. The stream function components were extended from $y/\delta_{1/2} = 2.4$ to $y/\delta_{1/2} = 4.0$ with a decaying exponential, as

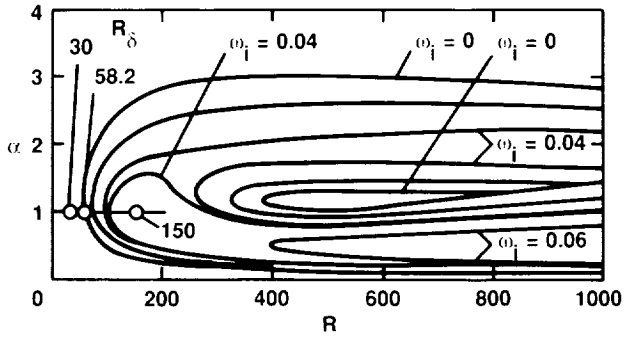

Figure 10. *Stability characteristics of the ideal wall jet (ref. 36).*

described by Chun and Schwarz. A typical disturbance streamline pattern for the wall jet is shown in figure 12, which shows the double-row vortex structure characteristic of the wall jet.

Wall-Jet Thermodynamic Stability

The disturbance velocity field was evaluated for these three conditions in order to compute the viscous dissipation function, which for incompressible, two-dimensional flow reduces to

$$\Phi = \mu\left[2\left(\frac{\partial u}{\partial x}\right)^2 + 2\left(\frac{\partial v}{\partial y}\right)^2 + \left(\frac{\partial v}{\partial x} + \frac{\partial u}{\partial y}\right)^2\right] \tag{60}$$

The mean-velocity derivatives, evaluated from the Glauert solution, are

$$\frac{\partial \bar{u}}{\partial y} = 3.1749 U_m f'' \tag{61a}$$

$$\frac{\partial \bar{u}}{\partial x} = \frac{\partial \bar{v}}{\partial y} = \frac{\partial \bar{v}}{\partial x} = 0 \tag{61b}$$

where

$$f'' = 2(g')^2 + 2gg'', \quad g'' = -g^2 g' \tag{62}$$

The velocity derivatives of the disturbance, evaluated from the disturbance stream function at $t = 0$, are

$$\frac{\partial u'}{\partial x} = -\frac{\partial v'}{\partial y} = \varepsilon\left[\alpha\varphi_r \cos(\alpha x) + \alpha\varphi_i \sin(\alpha x)\right] \tag{63a}$$

$$\frac{\partial u'}{\partial y} = \varepsilon\left[\frac{\partial^2 \varphi_r}{\partial y^2}\cos(\alpha x) - \frac{\partial^2 \varphi_i}{\partial y^2}\sin(\alpha x)\right] \tag{63b}$$

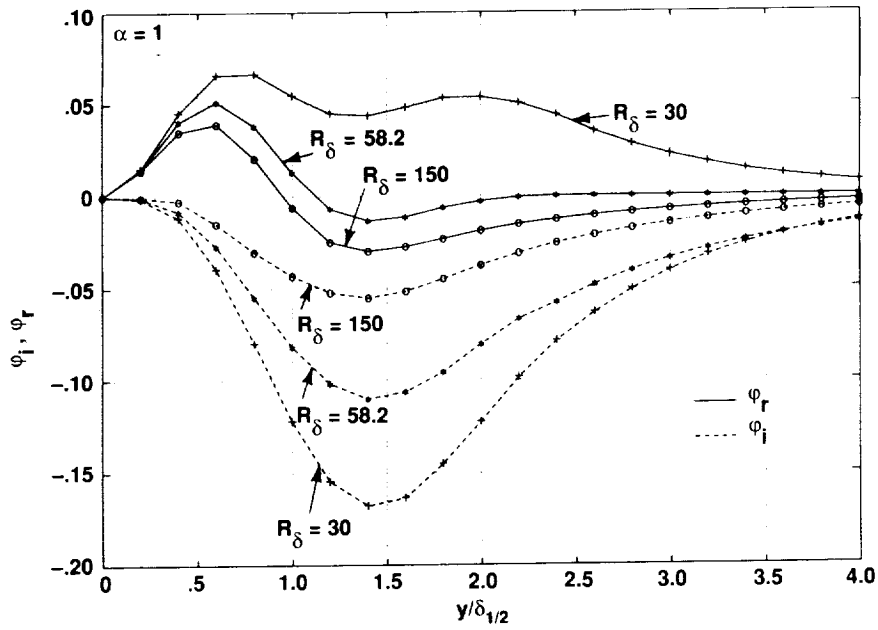

Figure 11. *Real and imaginary components of the disturbance stream function; α = 1, R_δ = 30, 58.2, 150 (ref. 35).*

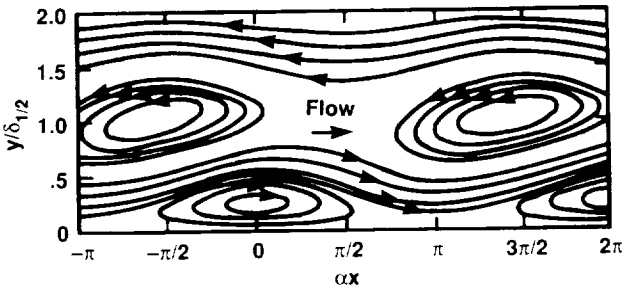

Figure 12. *Disturbance streamlines for an ideal wall jet; R = 200, c = 2 (ref. 36).*

$$\frac{\partial v'}{\partial x} = \varepsilon\left[\alpha^2\varphi_r\cos(\alpha x) - \alpha^2\varphi_i\sin(\alpha x)\right] \tag{63c}$$

Here, ε is a small parameter that is proportional to the amplitude of the disturbance. Negative values of ε are not permitted because they would violate the boundary conditions on the disturbance stream function. Errors associated with inaccuracies in the linearized equations for small but finite amplitude disturbances are neglected here.

The velocity derivatives of the mean and disturbed flow were used to evaluate the total viscous dissipation,

$$\Phi = \mu\left[2\left(\varepsilon\frac{\partial u'}{\partial x}\right)^2 + 2\left(\varepsilon\frac{\partial v'}{\partial y}\right)^2 + \left(\varepsilon\frac{\partial v'}{\partial x} + \frac{\partial \bar{u}}{\partial y} + \varepsilon\frac{\partial u'}{\partial y}\right)^2\right] \tag{64}$$

This expression was then integrated numerically over the region $0 < x/\delta_{1/2} < 4$ and $0 < y/\delta_{1/2} < 2\pi$ to evaluate the net dissipation. For this purpose, the integral was divided into three terms,

$$\iint_{A_v}\Phi dA_v$$

$$= \mu\iint_{A_v}\left(\frac{\partial \bar{u}}{\partial y}\right)^2 dA_v + 2\mu\varepsilon\iint_{A_v}\left[\frac{\partial \bar{u}}{\partial y}\left(\frac{\partial v'}{\partial x} + \frac{\partial u'}{\partial y}\right)\right]dA_v$$

$$+ \mu\varepsilon^2\iint_{A_v}\left[2\left(\frac{\partial u'}{\partial x}\right)^2 + 2\left(\frac{\partial v'}{\partial y}\right)^2 + \left(\frac{\partial v'}{\partial x} + \frac{\partial u'}{\partial y}\right)^2\right]dA_v \tag{65}$$

For a given condition of Reynolds number and wave number, the value of the net dissipation should vary quadratically with the disturbance amplitude and have positive curvature everywhere. The variation of net dissipation for the three Reynolds number conditions examined here is shown in figure 13. The variations of dissipation for negative values of disturbance amplitude are shown as dotted lines, since these variations violate the boundary conditions. If negative amplitudes were permitted, the corresponding vortical disturbances would rotate in the sense opposite to the actual disturbances.

Figure 13 shows that for R = 30, the condition associated with stable laminar flow, the value of the net dissipation increases with increasing disturbance amplitude. For R = 30, the minimum value of net dissipation is generated for vanishing disturbance amplitude, suggesting that this flow is stable thermodynamically as well as hydrodynamically. For R = 58, the case of neutral hydrodynamic stability, the curve of net dissipation has a horizontal tangent at the origin, suggesting that the flow is thermodynamically neutral for infinitesimal disturbances but stable for large disturbances. For R = 150, the net dissipation decreases as the disturbance amplitude increases from 0, until a minimum value of the net dissipation is reached at $\varepsilon = 0.005$. This suggests that the hydrodynamically unstable mean flow is also thermodynamically unstable, although the disturbed flow is thermodynamically stable for the value of $\varepsilon = 0.005$, at which the net dissipation is minimized. This situation may correspond to the nonlinear limit cycle that is sometimes observed in the real flow. Figure 14 shows a flow visualization of an initially laminar wall jet at R = 600; the large disturbances form a stable vortex array for many cycles in the downstream direction. Similar patterns form in the downstream wakes of cylinders or other bluff bodies (ref. 41). Such vortex arrays in an inviscid fluid show good agreement between predictions of stable motion and experimental results. Vortex arrays in a viscous fluid can also be considered from the standpoint of thermodynamic stability. This approach may contribute to the understanding of the discrete tone stabilization of separation-layer and boundary-layer control. In the next section, measurements of the velocity field of an unstable, initially laminar wall jet are used to estimate the components of the dissipation function in various regions of an unstable jet.

Dissipation in an Unsteady Wall Jet

To further consider dissipation effects in a real flow, it is convenient to separate the dissipation function into mean and fluctuating components. The components of pressure and vorticity are

$$p = \bar{p} + p', \quad \omega = \bar{\omega} + \omega' \tag{66}$$

so the dissipation function of equation (22) becomes

$$\tilde{\Phi}_I = -\frac{2\mu}{\rho}\nabla^2(\bar{p} + p') + \mu(\bar{\omega} + \omega')^2 \tag{67}$$

and the mean dissipation function is

$$\overline{\tilde{\Phi}}_I = -\frac{2\mu}{\rho}\nabla^2\bar{p} + \mu\left[(\bar{\omega})^2 + \overline{(\omega')^2}\right] \tag{68}$$

Figure 14 illustrates the periodic vortex motion of a two-dimensional wall-jet flow. This jet flow developed from an initially parabolic profile rather than a self-similar profile, which was considered in the preceding section.

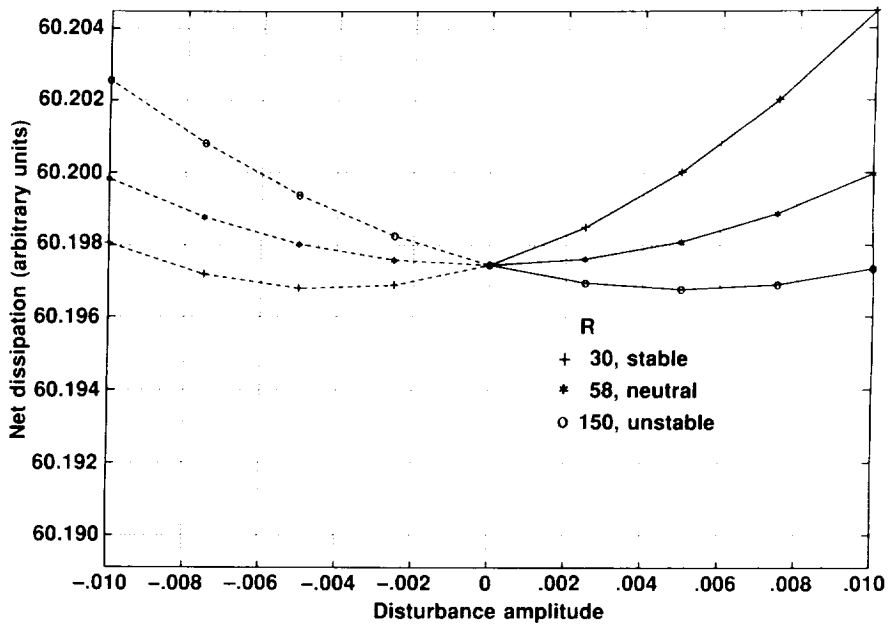

Figure 13. *Net dissipation integrated over $0 < x/\delta_{1/2} < 2\pi$ and $0 < y/\delta_{1/2} < 4.0$ vs. disturbance amplitude; R = 30, 58.2, 150.*

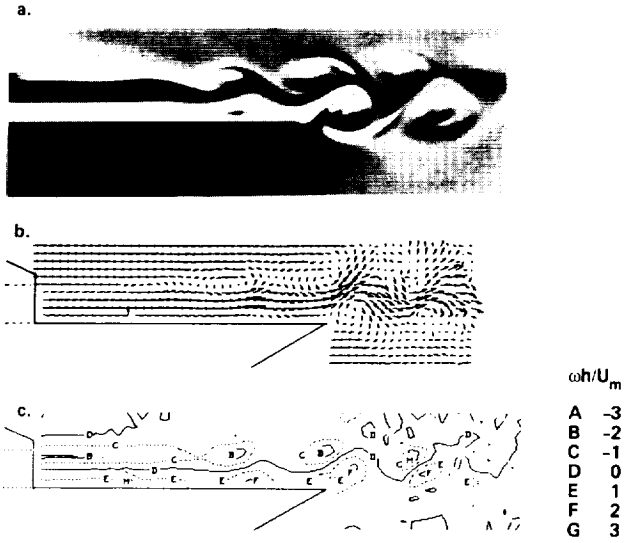

Figure 14. *Wall-jet phase-averaged velocity field and flow visualization; jet height = 0.508 cm, jet width = 10.16 cm, wall length = 3.81 cm, maximum velocity of the parabolic exit profile = 13.85 m/s, tone frequency = 600 Hz. a) Phase-averaged flow visualization, b) velocity vectors relative to convecting vortices, c) vorticity contours.*

Woolley and Karamcheti showed that the stability characteristics of nonparallel shear flows are closely related to those of parallel shear flows (ref. 42). The short wall was associated with the generation of tones by the jet; this tone generation significantly reduced the small-disturbance region by effectively forcing the initial jet region. However, the observed tone frequencies were approximately the same as those of the jet without forcing. The conditions for this jet are U_m = 13.85 m/s and L/h = 7.5, where U_m is the maximum velocity of the parabolic exit profile, L is the wall length, and h is the nozzle height. Figure 14(a) shows a phase-averaged schlieren visualization record obtained by lightly heating the subsonic nozzle flow. Figure 14(b) shows the phase-averaged velocity field, relative to the convecting vortices, and figure 14(c) depicts the corresponding vorticity field obtained with a central-differenced curl of the velocity field. The vorticity is normalized with respect to the maximum exit velocity and the nozzle height. We measured the velocity with a single x-wire velocity probe by sampling the probe output at regular phase intervals, which were determined by a pressure transducer fixed in the wall (ref. 43). The measurements were further processed to obtain estimates of the mean and fluctuating components of the dissipation field.

Relative contributions to the dissipative structure of the wall jet were estimated by integrating the field variables in the cross-stream direction. We define

$$I_T\left(\frac{x}{h}\right)=\left(\frac{h}{U_m}\right)^2\int\frac{\Phi}{\mu}d\left(\frac{y}{h}\right)=I_1+I_2+I_3 \qquad (69)$$

where

$$I_1=\left(\frac{h}{U_m}\right)^2\int-\frac{2}{\rho}\nabla^2\bar{p}\,d\left(\frac{y}{h}\right) \qquad (70a)$$

$$I_2=\left(\frac{h}{U_m}\right)^2\int\bar{\omega}^2\,d\left(\frac{y}{h}\right) \qquad (70b)$$

$$I_3=\left(\frac{h}{U_m}\right)^2\int(\omega')^2\,d\left(\frac{y}{h}\right) \qquad (70c)$$

The Laplacian of the pressure was computed from the divergence of the incompressible, viscous, two-dimensional momentum equation,

$$-\frac{2}{\rho}\nabla^2 p=2\left(\frac{\partial u}{\partial x}\right)^2+4\left(\frac{\partial u}{\partial y}\right)\left(\frac{\partial v}{\partial x}\right)+2\left(\frac{\partial u}{\partial y}\right)^2 \qquad (71)$$

To estimate the measurement error, the mean square of the divergence of the velocity was computed:

$$I_{div}=\left(\frac{h}{U_m}\right)^2\int\left(\frac{\partial u}{\partial x}+\frac{\partial v}{\partial y}\right)^2 d\left(\frac{y}{h}\right) \qquad (72)$$

This integral should vanish if the flow is two-dimensional and incompressible, and if measurements of u and v are accurate.

Figure 15 shows the distributions of I_1, I_2, I_3, I_{div}, and I_T for the jet conditions described. The measurement error indicated by I_{div} is negligible only upstream of the wall trailing edge, where the pressure Laplacian term, I_1, is also negligible. The square of the mean vorticity, I_2, is nearly constant in the small-disturbance region, $0 < x/h < 2.5$, beyond which it gradually decreases. Within the large-disturbance region, $2.5 < x/h < 7.5$, the net dissipation gradually increases with streamwise distance. The mean square of fluctuating vorticity, I_3, is negligible in the initial region, then steadily increases in the large-disturbance wall region. The decrease in I_T beginning at x/h = 2.5 is consistent with the decrease in net dissipation associated with hydrodynamically unstable flow that was noted in the preceding section.

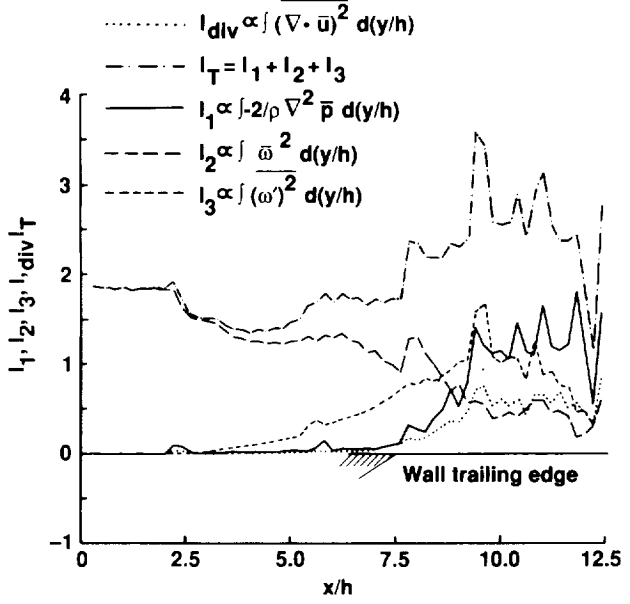

Figure 15. Distribution of integrated dissipation components.

These measurements demonstrate a method of directly measuring dissipative terms in an unsteady flow. This method can be extended to experimentally determine a relationship between overall dissipation and variable parameters such as forcing frequency, and to experimentally search for dissipation extrema.

CONCLUDING REMARKS

Many features of steady viscous fluid motion, such as the large extent of irrotational flow near streamlined bodies, are consistent with a thermodynamic interpretation based on the minimum dissipation of energy or production of entropy. Observations of this agreement have been made by various researchers over the last century; however, recent developments in the field of nonequilibrium thermodynamics justify further investigation along these lines. In this report, an exact equation was derived for the dissipation function of a homogeneous, isotropic, Newtonian fluid; the equation's terms are associated with irreversible compression or expansion, wave radiation, and the square of the vorticity. Simple flows, such as the incompressible channel flow and the cylindrical vortex, were identified as minimally dissipative distributions. A correspondence between hydrodynamic and thermodynamic stability is suggested by calculations and measurements of an initially laminar wall jet. These results suggest that the theory of nonequilibrium thermodynamics can serve to unify the understanding of many diverse phenomena in aerodynamics and aeroacoustics.

National Aeronautics and Space Administration
Ames Research Center
Moffett Field, California 94035-1000
June 27, 1990

REFERENCES

1. Batchelor, G. K.: An Introduction to Fluid Dynamics. Cambridge Univ. Press, 1973, pp. 227-228.

2. Tadmor, E.: A Minimum Entropy Principle in the Gas Dynamics Equations. NASA CR-178123, 1986.

3. Malkus, W. V. R.: Outline of a Theory of Turbulent Shear Flow. J. Fluid Mech., vol. 1, pt. 5, 1956, pp. 521-539.

4. Malkus, W. V. R.: Turbulent Velocity Profiles from Stability Criteria for Shear Boundary Layers. J. Fluid Mech., vol. 90, pt. 2, 1979, pp. 401-414.

5. Reynolds, W. C.; and Tiederman, W. G.: Stability of Turbulent Channel Flow, with Applications to Malkus's Theory. J. Fluid Mech., vol. 27, pt. 2, 1967, pp. 253-272.

6. Gage, D. H.; Schiffer, M.; Kline, S. J.; and Reynolds, W. C.: The Non-Existence of a General Thermokinetic Variational Principle. In: Non-Equilibrium Thermodynamics: Variational Techniques and Stability. ed. Donnely, R. J., Herman, R., and Prigogine, I., Univ. of Chicago Press, 1966, pp. 283-286.

7. Yourgrau, W.; van de Merwe, J.; and Raw, G.: Treatise on Irreversible and Statistical Thermodynamics. Macmillan, Inc., 1966.

8. de Groot, S. R.; and Mazur, P: Non-Equilibrium Thermodynamics. Dover, 1984.

9. Onsager, L.: Reciprocal Relations in Irreversible Processes. Phys. Rev., vol. 37, no. 2, 1931, pp. 405-426.

10. Prigogine, I.: Introduction to Thermodynamics of Irreversible Processes. 3rd ed. Wiley Interscience, 1967.

11. Prigogine, I.: From Being to Becoming. W. H. Freeman and Co., 1980.

12. Prigogine, I.; and Stengers, I.: Order Out of Chaos. Bantam Books, 1984.

13. Busse, F. H.: The Stability of Finite Amplitude Cellular Convection and its Relation to an Extremum Principle. J. Fluid Mech., vol. 30, pt. 4, 1967, pp. 625-649.

14. Paltridge, G. W.: Thermodynamic Dissipation and the Global Climate System. Royal Meteorological Society, Quarterly Journal, vol. 107, no. 453, July 1981, pp. 531-547.

15. Casas-Vazquez, J.; and Lebon, G., eds.: Stability of Thermodynamic Systems. Lecture Notes in Physics, no. 164. Springer-Verlag, 1982.

16. Lugt, H. L.: Vortex Flows in Nature and Technology. Wiley and Sons, Inc., 1983.

17. Ziegler, H.: An Introduction to Thermomechanics. North-Holland Publ. Co., 1983, pp 253-269.

18. Jeffreys, H.: Cartesian Tensors. Cambridge Univ. Press, 1974, pp. 84-89.

19. Phillips, O. M.: On the Generation of Sound by Supersonic Turbulent Shear Layers. J. Fluid Mech., vol. 9, no. 1, 1960, pp. 1-28.

20. Horne, W. C.; and Karamcheti, K.: Extrema Principles of Entropy Production and Energy Dissipation in Fluid Mechanics. NASA TM-100992, 1988.

21. Lighthill, M. J.: On Sound Generated Aerodynamically: I. General Theory. Proc. Roy. Soc., vol. 211A, no. 1107, 1952, pp. 564-587.

22. Shapiro, A.: The Dynamics and Thermodynamics of Compressible Flow. Ronald Press Co., 1953.

23. Leith, C. E.: Minimum Enstrophy Vortices. Phys. Fluids, vol. 27, no. 6, June 1984, pp. 1388-1395.

24. Hinze, J.: Turbulence. 2nd ed. McGraw-Hill, 1975.

25. Tennekes, H.; and Lumley, J. L.: A First Course in Turbulence. MIT Press, 1972, p. 88.

26. Elsgolc, L. E.: Calculus of Variations. Pergamon, 1962.

27. Yates, J. E.; and Donaldson, C. duP.: A Fundamental Study of Drag and an Assessment of Conventional Drag-Due-to-Lift Reduction Devices. NASA CR-4004, 1986.

28. Greene, G. C.: An Entropy Method for Induced Drag Minimization. SAE-892344, Sept. 1989.

29. von Karman, T.: Problems of Flow in Compressible Fluids. In: Fluid Mechanics and Statistical Methods. University of Pennsylvania Bicentennial Conference, Univ. of Penn. Press, 1941, pp. 15-39.

30. Abbot, I. H.; and von Doenhoff, A. E.: Theory of Wing Sections. Dover, 1959.

31. Yates, J. E.: Viscous Thin Airfoil Theory. NASA CR-163069, 1980.

32. Lagerstrom, P. A.: Laminar Flow Theory. In: High Speed Aerodymamics and Jet Propulsion, Vol. 4: Theory of Laminar Flows. Princeton Univ. Press, 1964.

33. Thwaites, B.: Incompressible Aerodynamics. Clarendon Press, 1960, p. 179.

34. Betchov, R.; and Criminale, W. O.: Stability of Parallel Flows. Academic Press, 1967.

35. Chun, D. H.; and Schwarz, W. H.: Stability of the Plane Incompressible Viscous Wall Jet Subjected to Small Disturbances. Physics of Fluids, vol. 10, no. 5, 1967, pp. 911-915.

36. Tsuji, Y.; Morikawa, Y.; Nagatani, T.; and Sakou, M.: The Stability of a Two-Dimensional Wall Jet. Aeronautical Quarterly, vol. 28, pt. 4, 1977, pp. 235-246.

37. Vanderborck, G.; and Platten, J. K.: Stability of the Pipe Poiseuille Flow, With Respect to Axi and Nonaxisymmetric Disturbances. J. Non-Equil. Thermodyn., vol. 3, 1978, pp. 169-190.

38. Glansdorff, P.; and Prigogine, I.: On a General Evolution Criterion in Macroscopic Physics. Physica, vol. 30, no. 2, 1964, pp. 351-374.

39. Marsik, F.: Thermodynamic Approach to Stability of Transonic Flow and its Numerical Solution. J. Non-Equil. Thermodyn., vol. 14, no. 4, 1989, pp. 299-314.

40. Glauert, M. B.: The Wall Jet. J. Fluid Mech., vol. 1, pt. 6, 1956, pp. 625-643.

41. Zdravkovich, M. M.: Smoke Observations of the Formation of a Karman Vortex Street. J. Fluid Mech., vol. 37, pt. 3, 1969, pp. 491-496.

42. Woolley, J. P.; and Karamcheti, K.: The Role of Jet Stability in Edgetone Generation. AIAA Paper 73-628, July 1973.

43. Horne, W. C.: Measurements of Large Scale Disturbances in Rectangular Wall Jets. AIAA Paper 84-2314, Oct. 1984.

NASA
National Aeronautics and Space Administration

Report Documentation Page

1. Report No.	2. Government Accession No.	3. Recipient's Catalog No.
NASA TP-3118		

4. Title and Subtitle	5. Report Date
Aeroacoustic and Aerodynamic Applications of the Theory of Nonequilibrium Thermodynamics	June 1991
	6. Performing Organization Code

7. Author(s)	8. Performing Organization Report No.
W. Clifton Horne, Charles A. Smith, and Krishnamurty Karamcheti	A-90084
	10. Work Unit No. 505-61-00

9. Performing Organization Name and Address	11. Contract or Grant No.
Ames Research Center Moffett Field, CA 94035-1000	
	13. Type of Report and Period Covered Technical Paper

12. Sponsoring Agency Name and Address	14. Sponsoring Agency Code
National Aeronautics and Space Administration Washington, DC 20546-0001	

15. Supplementary Notes

Point of Contact: W. Clifton Horne, Ames Research Center, MS 247-2, Moffett Field, CA 94035-1000
(415) 604-4571 or FTS 464-4571
W. Clifton Horne and Charles A. Smith: Ames Research Center, Moffett Field, California.
Krishnamurty Karamcheti: FAMU-FSU College of Engineering, Tallahassee, Florida.

16. Abstract The objective of this report is to examine recent developments in the field of nonequilibrium thermodynamics associated with viscous flows, and to relate these developments to the understanding of specific phenomena in aerodynamics and aeroacoustics. A key element of the nonequilibrium theory is the principle of minimum entropy production rate for steady dissipative processes near equilibrium, and variational calculus is used to apply this principle to several examples of viscous flow. The paper begins with a review of nonequilibrium thermodynamics and its role in fluid motion. Several formulations are presented of the local entropy production rate and the local energy dissipation rate, two quantities that are of central importance to the theory. These expressions and the principle of minimum entropy production rate for steady viscous flows are used to identify parallel-wall channel flow and irrotational flow as having minimally dissipative velocity distributions. Features of irrotational, steady, viscous flow near an airfoil, such as the effect of trailing-edge radius on circulation, are also found to be compatible with the minimum principle. Finally, the minimum principle is used to interpret the stability of infinitesimal and finite amplitude disturbances in an initially laminar, parallel shear flow, with results that are consistent with experiment and linearized hydrodynamic stability theory. These results suggest that a thermodynamic approach may be useful in unifying the understanding of many diverse phenomena in aerodynamics and aeroacoustics.

17. Key Words (Suggested by Author(s))	18. Distribution Statement
Minimum dissipation Aerodynamic flows Thermodynamic stability	Unclassified-Unlimited Subject Category - 34

19. Security Classif. (of this report)	20. Security Classif. (of this page)	21. No. of Pages	22. Price
Unclassified	Unclassified	28	A03

NASA FORM 1626 OCT 86

For sale by the National Technical Information Service, Springfield, Virginia 22161

NASA-Langley, 1991